②

REPORT DOCUMENTATION PAGE	Form Approved OMB No. 0704-0188

1a. REPORT SECURITY CLASSIFICATION Unclassified	1b. RESTRICTIVE MARKINGS

DTIC ELECTED
PR 1 4 1989

AD-A206 839

	3. DISTRIBUTION/AVAILABILITY OF REPORT Approved for public release; distribution is unlimited.

5. MONITORING ORGANIZATION REPORT NUMBER(S) AFOSR·TR· 89-0405

6a. NAME OF PERFORMING ORGANIZATION The Pennsylvania State University	6b. OFFICE SYMBOL (If applicable)	7a. NAME OF MONITORING ORGANIZATION AFOSR/NA
6c. ADDRESS (City, State, and ZIP Code) University Park, PA 16802		7b. ADDRESS (City, State, and ZIP Code) Building 410, Bolling AFB DC 20332-6448
8a. NAME OF FUNDING/SPONSORING ORGANIZATION AFOSR/NA	8b. OFFICE SYMBOL (If applicable) NA	9. PROCUREMENT INSTRUMENT IDENTIFICATION NUMBER AFOSR-87-0145

8c. ADDRESS (City, State, and ZIP Code) Building 410, Bolling AFB DC 20332-6448	10. SOURCE OF FUNDING NUMBERS			
	PROGRAM ELEMENT NO. 61102F	PROJECT NO. 2308	TASK NO. A2	WORK UNIT ACCESSION NO.

11. TITLE (Include Security Classification)

(U) "Fuel Structure and Pressure Effects on the Formation of Soot Particles in Diffusion Flames"

12. PERSONAL AUTHOR(S)
Robert J. Santoro

13a. TYPE OF REPORT Annual Technical	13b. TIME COVERED FROM 1/15/88 TO 1/15/89	14. DATE OF REPORT (Year, Month, Day) 1989, February, 15	15. PAGE COUNT 37

16. SUPPLEMENTARY NOTATION

17. COSATI CODES			18. SUBJECT TERMS (Continue on reverse if necessary and identify by block number)
FIELD	GROUP	SUB-GROUP	Soot Formation, Soot Particles, Diffusion Flames

19. ABSTRACT (Continue on reverse if necessary and identify by block number)

Studies emphasizing the effects of fuel molecular structure on soot formation processes in laminar diffusion flames have been investigated. Particular attention has been given to the particle inception and surface growth processes for a series of fuels. Studies of butane, 1-butene and 1,3 butadiene have revealed that fuel structure strongly affects the soot particle inception process. However, subsequent surface growth processes are largely determined by the available surface area. Thus, the surface growth process is independent of the fuel molecular structure following the initial particle inception stage. Studies of the particle inception region indicate that increased soot formation is strongly correlated with visible fluorescence measurements attributed to large polynuclear aromatic hydrocarbon species in the flame. Attempts to quantitatively evaluate the potential contribution of such species to early particle growth were not conclusive. In addition to these atmospheric flame studies, an investigation of soot formation in high pressure diffusion flames was also initiated. Results to date indicate general agreement with previous studies of the pressure dependence of soot formation processes. Thus, the present studies represent the first independent verification of this observed dependence.

20. DISTRIBUTION/AVAILABILITY OF ABSTRACT ☒ UNCLASSIFIED/UNLIMITED ☒ SAME AS RPT. ☒ DTIC USERS	21. ABSTRACT SECURITY CLASSIFICATION Unclassified
22a. NAME OF RESPONSIBLE INDIVIDUAL Julian M Tishkoff	22b. TELEPHONE (Include Area Code) (202)767- 22c. OFFICE SYMBOL AFOSR/NA

DD Form 1473, JUN 86   Previous editions are obsolete.   SECURITY CLASSIFICATION OF THIS PAGE

Annual Report

on

Fuel Structure and Pressure Effects on the Formation
of Soot Particles in Diffusion Flames

(AFOSR Contract   AFOSR-87-0145)

Prepared by

Robert J. Santoro
Department of Mechanical Engineering
The Pennsylvania State University
University Park, PA   16802

Submitted to:

Air Force Office of Scientific Research
Bolling Air Force Base
Washington, D.C.

March 1989

TABLE OF CONTENTS

SUMMARY

Studies emphasizing the effects of fuel molecular structure on soot formation processes in laminar diffusion flames have been investigated. Particular attention has been given to the particle inception and surface growth processes for a series of fuels. Studies of butane, 1-butene and 1,3 butadiene have revealed that fuel structure strongly affects the soot particle inception process. However, subsequent surface growth processes are largely determined by the available surface area. Thus, the surface growth process is independent of the fuel molecular structure following the initial particle inception stage. Studies of the particle inception region indicate that increased soot formation is strongly correlated with visible fluorescence measurements attributed to large polynuclear aromatic hydrocarbon species in the flame. Attempts to quantitatively evaluate the potential contribution of such species to early particle growth were not conclusive. In addition to these atmospheric flame studies, an investigation of soot formation in high pressure diffusion flames was also initiated. Results to date indicate general agreement with previous studies of the pressure dependence of soot formation processes. Thus, the present studies represent the first independent verification of this observed dependence.

1. INTRODUCTION

Recent interest in the formation of soot in combustion processes has been motivated by several related developments. It is now well recognized that future combustion systems will operate with broader specification fuels under conditions of higher operating pressures and stricter emissions standards. Each of these developments requires appropriate optimization of combustion processes and system performance capabilities; increase soot formation represents a major challenge in this process. Since soot production has been shown to have strong sensitivity to fuel properties and operating conditions (temperature and pressure) [1,2], it would be desirable to have an understanding of the fundamental processes governing soot formation and subsequent oxidation. However, such understanding must also be developed under conditions which can be directly extended to processes occurring in practical combustion systems. The objective of the present effort is to investigate the effects of fuel molecular structure and operating pressure on the rates of soot formation, particle growth and burnout in a well characterized flow field. These results are expected to provide an understanding of the fundamental processes involved in soot formation under conditions which are characteristic of practical combustion systems.

2. RESEARCH OBJECTIVE

The objective of the present study is to provide an understanding of the effects of fuel molecular structure and operating pressure on the formation of soot particles in combustion systems. These studies are carried out in a series of laminar diffusion flames and require extensive characterization of the particle, velocity and temperature fields present in these flames. Studies are conducted at both atmospheric and elevated pressures in order to examine the effect of pressure on both the formation and oxidation of soot particles. A coannular diffusion flame apparatus is used to study the soot formation processes in these gaseous flames. The coannular burner has been selected as the experimental burner because of its demonstrated capability to produce stable flames over a wide range of operating conditions [3,4,5]. Pressure is known to exert a significant effect on soot particle formation. High pressure flame studies are carried out in a flame facility assembled for this work which has the capability to operate at pressures as high as twenty atmospheres.

The effect of fuel structure is studied by the addition of aliphatic hydrocarbons (e.g., butane, butene, butadiene) and aromatics (e.g., alkylated benzenes, naphthalenes and naphthenes) in various proportions to well characterized diffusion flames. Effects of such characteristic compounds are examined using previously well characterized ethene and methane diffusion flames. These efforts can be supplemented with studies of prevaporized fuels (e.g., pentane, decane) and include blends with characteristic aromatic species. The effect that temperature has on soot formation and oxidation will also be investigated in these flames. Inert species (e.g., nitrogen and argon) can be added to either the fuel or oxidizer flow to vary the effective flame temperature. Previous studies using this approach have established the strong sensitivity of soot particle formation and destruction processes to temperature [4,6]. Using the measured particle volume fraction, size and number density, it will be possible to examine the temperature dependence of the rates of initial formation, growth and subsequent oxidation of the soot particles.

The measurement approaches stress the use of non-intrusive optical diagnostic techniques. Laser based techniques, such as laser light scattering and laser anemometry, are used to measure physical properties of the soot particles and to characterize the fluid velocity field. At present, fine wire thermocouple measurements are used to determine the temperature field.

The essential thrust of this research effort is to obtain soot particle formation, growth and burnout rates using non-intrusive techniques so as to leave unaltered the dynamic coupling of the chemical and fluid mechanical processes. The operating conditions of the flames studied and fuels investigated are intended to be characteristic of the conditions to be encountered in future gas turbine systems. The consideration of gaseous and prevaporized fuels avoids the complications that spray combustion diagnostics introduce to the study of soot formation, while preserving the consideration of realistic fuel constituents in the study. Such studies should complement work being undertaken to elucidate chemical precursor mechanisms as well as those concerned with more global

measurements of soot production such as soot mass yield.

The detailed nature of the results of this study, as well as the tractable nature of the flame environment, will provide an important addition to the data base available for combustion model validation. Our approach will be to use existing models developed for conditions appropriate for laminar diffusion flames [7] and build on their capabilities to include the important particle processes [8]. Efforts will also be made to collaborate with modeling approaches being attempted elsewhere [9]. Since the proposed experiments will consider a range of chemical structures under varying pressure and temperature conditions, this work will offer an opportunity for model development over a wide range of conditions.

3. EXPERIMENTAL FACILITIES

Before presenting the accomplishments and status of the research program, it is useful to describe the experimental facilities which have been utilized in these studies. These facilities were assembled during the first year of the program and were previously described in last year's annual report. These facilities include the atmospheric and high pressure diffusion flame burners, the laser light scattering apparatus and the laser velocimeter system.

3.1 Atmospheric Diffusion Flame Facility

The atmospheric diffusion flame facility consists of coannular diffusion flame burner, burner chimney, positioning system and gas metering system. The burner has a coannular configuration consisting of a 1.1 cm fuel tube surrounded by a 10 cm air annulus. The air passage is partially filled with glass beads followed by a series of fine screens to provide flow conditioning. A ceramic honeycomb 2.54 cm in thickness is used at the exit to provide a uniform flow field. The fuel tube which extends 4.8 mm above the ceramic honeycomb also is partly filled with glass beads to condition the flow. The fuel flow can consist of up to three gases, each metered with a separate rotameter. This allows for mixtures of fuels as well as nitrogen dilution of the fuel for temperature control. These rotameters have been calibrated for various gases using a soap bubble meter technique. The air flow is metered using a mass flowmeter which can monitor flows up to 5 SCFM of air. To protect the flame from room disturbances, a metal chimney has been incorporated into the burner facility. This chimney translates horizontally with the burner while sliding vertically within the chimney. Slots machined in the chimney provide for optical access.

The burner is mounted on a pair of motorized translating stages which provide for vertical and horizontal motion. A manual translation stage is also included to allow for adjustment in the second horizontal direction and is used to align the burner with the laser scattering system. The motorized stages are used to traverse the burner through the laser beam to obtain measurements over the cross section of the flame at a particular height in the flame. The motorized translation stages have a positioning resolution of 0.0127 mm which is sufficient for the present experiments. Both motorized stages are interfaced to and controlled by an IBM-XT computer using the general purpose interface bus (GPIB-IEEE 488). The software to control the translation stages is incorporated into the data acquisition program for the laser scattering measurements.

3.2 High Pressure Diffusion Flame Facility

In order to provide for studies at elevated pressure, a high pressure diffusion flame facility has been constructed. This facility is composed of a coannular burner, pressure vessel, positioning system and gas metering apparatus. The design chosen provides for a significant degree of similarity between the atmospheric and high pressure diffusion flame burners. A burner identical to that previously described in section 3.1 has been constructed. This burner is mounted inside a high pressure vessel capable of withstanding the required operating pressures. The high pressure diffusion flame burner is shown in Figure 1.

KEY:

PRESSURE VESSEL
TRANSLATION ASSEMBLIES
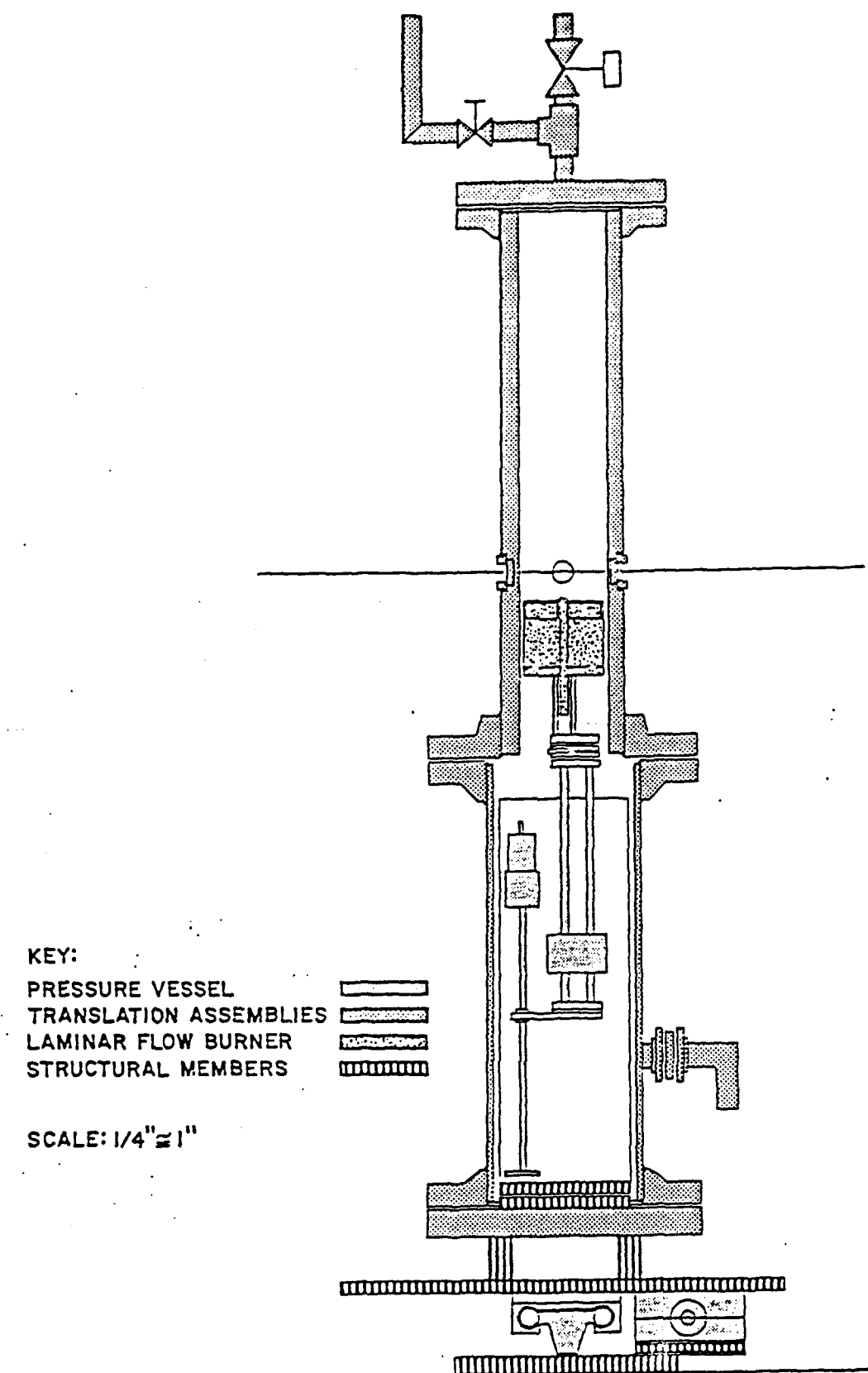LAMINAR FLOW BURNER
STRUCTURAL MEMBERS

SCALE: 1/4"≅1"

Figure 1. High Pressure Diffusion Flame Burner

Because of the mass of the pressure vessel, the approach chosen for the atmospheric system of vertically translating the entire burner and pressure vessel is not feasible. Rather the burner is mounted on a motorized translation stage located internal to the pressure vessel. Electrical connections are made through the base of the pressure vessel allowing external control of the burner's vertical position. To provide horizontal movement, the base of the pressure vessel is attached to a precision ball bearing stage which requires only a few pounds of force to move horizontally with weights as large as 1500 pounds attached. Thus, a relatively small motorized translation stage can be used to provide horizontal movement. As with the atmospheric burner, these motorized stages are capable of computer control using the laboratory IBM-XT personal computer. The only disadvantage with its approach is that sufficient space must be provided within the pressure vessel to house the vertical motion assembly and the flexible gas supply lines for the burner.

To accommodate this approach, the pressure vessel has been constructed as two separate sections. The lower section is constructed of 8 inch diameter schedule 40 carbon steel seamless pipe which is 24 inches in length. A 2 inch diameter schedule 40 carbon steel pipe is mounted and welded to this section to mount a diaphragm burst disc assembly. The burst disc is one of several safety features incorporated into the design of the burner. The vertical translating mechanism is mounted to the base of this lower section which is constructed of an 8 inch (300 lb class) blind flange. In addition to the electrical connection for the motorized translation stage, provisions for connection of fuel and air lines are also made through this flange. Internal connections to the diffusion flame burner can be made with low pressure tygon tubing since no pressure difference exists across the tubing wall inside the pressure vessel. With the upper section removed, access to the burner is easily afforded.

The upper section of the pressure vessel, which provides for optical access to the flame region, is 30 inches in length and is constructed from schedule XX 6 inch diameter carbon steel pipe. The wall thickness afforded by schedule XX pipe (0.864 inches) is required because of the four large diameter windows mounted into this section. These windows are two inches in diameter and 1/2 inch thick. These large diameter windows allow sufficient optical access for both the laser light scattering and the laser velocimetry measurements. In addition to the windows, access has been provided to allow igniting the flame through a 1/2 inch NPT hole in the bottom of this section. Near the top, 1/4 inch NPT holes are provided to monitor the temperature and pressure.

The operating pressure in the burner is adjusted presently using manual valves located in the exhaust line of the burner. Connection to this exhaust system is made through a second blind flange to which a 2 inch diameter exhaust line has been connected. Presently consideration is being given to replacing this manual system with a back pressure regulator which allows for better pressure control. At this time, no cooling is required for the burner or exhaust section. Temperature measurements indicate that for conditions typical for the present experiments, the burner does not heat up significantly.

Control and measurement of the fuel and air flow rates is accomplished using mass flow meters and controllers. These meters are insensitive to the operating pressure and thus can be calibrated at atmospheric pressure while providing accurate metering at elevated pressure. The fuel metering system allows up to three gases to be mixed using independent mass flow controllers. These controllers maintain a constant mass flow independent of the pressure drop across the meter. This assures a constant mass flow rate of fuel as well as a convenient start-up capability. Otherwise, the fuel flow rate would decrease as the operating pressure was increased, requiring continual readjustment. Because of the relatively large air flow rate required, a mass controller approach is not feasible for the air metering. The air flow rate is monitored by a mass flowmeter which requires adjustment as the operating pressure is varied.

3.3 Laser Light Scattering Apparatus

The laser light scattering apparatus, utilizing a 4W argon ion laser as the light source, provides for particle extinction and scattering measurements. Scattering measurements are presently made primarily at 90° although the system can be used to obtain measurements at 45° and 135°. The laser

source is modulated using a mechanical chopper operating at 1 kHz to allow for synchronous detection of the transmitted and scattered light signals. A polarization rotator is also incorporated in the system to allow adjustment of the polarization of the incident light beam. The laser beam is focused in the burner using a 30 cm focal length lens which results in a probe beam diameter of 0.02 cm. Typically the laser is operated at the 514.5 nm laser line with an output power of about 0.5W.

The transmitted light signal is detected using a silicon photodiode. The laser light intensity is reduced by a neutral density filter (N.D.≈2.0) to a level suitable for linear photodiode response. The scattered light is detected using a photomultiplier detector (PMT). The PMT has a narrowband filter center at 514.5 nm with a 1 nm bandwidth incorporated in the PMT housing to help reject light other than that generated from the particle scattering event. A pinhole with a diameter of 1 mm located in front on this filter limits the measurement volume length along the beam to 0.1 cm. The 15 cm focal length collection lens used to focus the scattered light onto the PMT, is arranged to provide unity magnification. Thus, the collection volume is a cylinder approximately 0.02 cm in diameter and .1 cm in length resulting in a volume of 3.1×10^{-3} cm^3. The collection lens is preceded by a polarization filter to allow polarization discrimination for the scattered light detected. The collection solid angle is determined by a 1.27 cm aperture which is located between the polarization filter and the collection lens. This aperture limits to the collection angle to approximately 2°.

The output from each of the detectors is input into separate two phase lock-in amplifiers which are interfaced to the IBM-XT computer over the GPIB bus. These units are capable of full computer control which allows for autoranging of the lock-in amplifiers. Computer software to control the lock-in amplifiers has been integrated with the stepper motor control programs to provide a complete data acquisition routine. These procedures provide a high degree of user independent data acquisition.

Data taken from the lock-in amplifiers is stored on the IBM-XT internal disk. The light scattering measurements require extensive data reduction to yield particle size information. Such calculations are performed more expeditiously on computers more capable than the laboratory computer used for the data acquisition. Thus, the IBM-XT is linked over the Mechanical Engineering Department's network to the University's VAX computer facilities. This allows for rapid data analysis and graphical output. The necessary data reduction and plotting software have been developed for this facility. In addition, the latest version of the NASA Equilibrium code has also been implemented on the VAX computer. The equilibrium program is used to calculate the adiabatic flame temperature for the diffusion flame studies.

The scattered light detection system is calibrated to account for effects of the incident laser power, sample volume, light collection efficiency, photomultiplier sensitivity and electronic gain of the system. The calibration is accomplished by passing ethene, a gas with a known Rayleigh scattering cross section, through the fuel passage of the burner and measuring the resulting scattered light. This procedure allows for an absolute determination of the differential scattering cross section per unit volume, $Q(\theta)$, which is the power scattered in the direction θ per unit incident flux. For these calibrations the incident laser beam is vertically polarized and θ is usually 90°.

The laser light scattering and extinction apparatus provides the particle measurement capability for the present studies. Analysis of the scattering measurements is based on a MIE theory approach for spherical particles. For completeness, a brief review of the theoretical basis for this analysis is presented. The present data reduction programs mentioned earlier incorporate the approach described below to obtain particle size and concentration information.

In general, the interaction of a particle and light wave is dependent on:

1. index of refraction of the particle, m

2. particle size, D

3. particle number density, N

4. particle size distribution, P(D)

5. particle shape

6. wavelength of the scattered light

7. scattering geometry

Obviously, measurement of any one of the above requires knowledge of all of the other variables. In a typical combustion measurement of soot particles, only the scattering geometry and the wavelength of the light can be specified beforehand. The remaining unknowns are determined by an appropriate combination of measurements to reduce the number of free parameters along with some reasonable assumptions. It is these assumptions which can result in inaccuracies and therefore must be considered carefully.

Combinations of scattering measurements utilizing the angular and polarization dependencies of the scattering process, or scattering and absorption measurements, have been used to determine particle number density and size [3-5]. In such an approach, the index of refraction is taken to be known, the particles are assumed to be spherical and a size distribution is assumed (e.g., log-normal).

The determination of particle size and number concentration from light scattering data depends primarily on our capability to relate the measurement of scattered and absorbed light intensity to the particle properties. Appropriate theories have been developed for spherical particles and have been widely applied for aerosol measurements. The particle properties of interest are the differential scattering cross section, $C_{ij}(\theta)$, for production of scattered light at a specified direction and total cross section for a specified particle size, C_{ext}. The subscripts i and j for the scattering cross section assume letters v or h according to whether the state of polarization of the scattered (i) and incident (j) radiation is perpendicular or parallel, respectively, to the plane of observation. For spherical particles of isotropic material, only the case of i ≈ j is of interest because cross polarization effects are absent.

The relationship between these cross sections and the experimentally measured quantities are expressed as

$$I_s = I_o N C_{ij} \left(\theta, \frac{\Pi D}{\lambda}, m\right) G \tag{1}$$

and

$$\frac{I}{I_o} = \exp -\int_O^L N C_{ext} \left(\frac{\Pi D}{\lambda}, m\right) ds \tag{2}$$

where I_s, I and I_o are the scattered, transmitted and incident intensities respectively, N is number concentration of particles, D is diameter, m is the refractive index, and G is a constant which involves factors related to the sample volume and detection instrumentation. It should be noted that the scattering cross section measurements given by equation (1) are point measurements, while the extinction cross section is an integrated quantity over the path length L. Thus, to obtain local particle extinction values, a data inversion technique must be utilized [10].

In an experiment, the quantities which are determined, once appropriate calibration factors have been introduced, are

$$Q_{ii} = N \, C_{ii} \tag{3}$$

and

$$K_{ext} = N \, C_{ext} \tag{4}$$

where Q_{ii} is the volumetric scattering cross section and K_{ext} is the extinction coefficient [11].

Several approaches can be taken to determine the particle size from the above defined cross sections. Three are of interest with respect to the instrumental set up discussed previously. These are the ratio of scattering to extinction, $Q_{vv}(90°)/K_{ext}$, the ratios of the scattering signal at two angles (dissymmetry ratio) $Q_{vv}(45°)/Q_{vv}(90°)$ and $Q_{vv}(45°)/Q_{vv}(135°)$, and the polarization ratio $Q_{hh}(90°)/Q_{vv}(90°)$; the scattering measurement angle is specified for each quantity. Each of these ratios have a strong dependence on particle size and represent a redundant set of data in terms of the particle properties for particles in the Mie size region ($D > \lambda$). For particles in the Rayleigh size region ($D \ll \lambda$), scattering is isotropic so the dissymmetry ratio has a value of unity and the defined polarization ratio approaches zero. Thus, in this small particle limit, only the scattering/extinction ratio yields size information. However, for soot formation processes, the rapid coagulation and surface growth processes lead quickly to particles in the Mie region. Nonetheless, the scattering measurement capabilities described above, provide for the measurement of the particle size throughout the Rayleigh and Mie regimes. Thus, processes from nucleation through particle growth and eventual particle oxidation are measurable.

With the particle size established, any one of the scattering cross sections can be used to find N or f_v, the soot volume fraction. The soot volume fraction, particle size and number density are related by

$$f_v = \frac{N\pi D^3}{6} \tag{5}$$

For a system in which simultaneous nucleation, particle growth and coagulation are present, a particle size distribution can be assumed to exist. In this case, the previously defined particle scattering cross sections must be averaged over the size distribution function, P(D), to yield mean values,

$$C_{ii}(\theta) = \int_0^\infty C_{ii}(\theta, \frac{\pi D}{\lambda}, m) \, P(D) \, dD \tag{6}$$

$$C_{ext} = \int_0^\infty C_{ext}(\frac{\pi D}{\lambda}, m) \, P(D) \, dD \tag{7}$$

A widely used expression for P(D) is the logarithmic normal distribution that is given by

$$P(D) = \frac{\exp[-(\ln D/D_g)^2/2\,\sigma_g^2]}{\sqrt{2\pi}\,\sigma_g D} \tag{8}$$

where D_g and σ_g are the geometric mean diameter and geometric mean standard deviation, respectively. As is discussed in Ref. 12, the introduction of particle size distribution affords an opportunity to derive additional information by utilizing the previously redundant measurements of the scattering cross sections. These now afford the possibility of learning more about the nature of the size distribution function and agglomerate particle properties.

4. ACCOMPLISHMENTS AND STATUS OF WORK

During the past yer;, studies have concentrated on several areas of the soot formation problem. Both atmospheric and high pressure laminar diffusion flames have been investigated. Studies have concentrated on both the particle inception and surface growth regions for the atmospheric flames. In the case of the high pressure flames, a series of studies involving ethene flames have been completed to assess the effect of pressure on the soot formation process. In the course of the high pressure studies, an interesting flame instability phenomena has been observed which has been investigated to an extent as well.

Specifically the following tasks have been accomplished:

1. In order to begin to better understand the relationship between the soot precursor chemistry and the inception of soot particles, an investigation of the early particle formation region has been undertaken. Using laser light scattering measurements for soot particle characterization and laser fluorescence measurements for large hydrocarbon species determination, a comparison of the particle inception region for a series of fuels has been investigated. The fuels investigated include butane, 1-butene and 1,3 butadiene introduced into a methane baseline flame. The results of these studies clearly show a strong correlation between the fluorescence observed from gas phas:: species and the early soot particle inception and growth rates. It is hoped that these results will form a basis for comparison of these laminar diffusion flame results with detailed chemical kinetic models of soot formation.

2. In these same flames, comparisons between the specific surface growth rates for the C_4 fuels studied have been made. These studies show that when the available surface area of the soot particles is taken into account, the specific surface growth rate constant is similar for all of the flames. This result further emphasizes the importance of the inception process, since initial surface area determines the subsequent growth of the soot particles.

3. In the studies described above, a detailed determination of the velocity field is required in order to determine the particle paths in the flame. Presently measurements obtained in a similar ethene/air diffusion flame have been used to complete the analysis. Although these results represent a good first approximation to the velocity field, it is desirable to have the velocity field for the specific flame under study. To this end, velocity measurements in the butane/methane and 1-butene/methane flames have been obtained. Analysis of these velocity measurements is presently underway. Comparisons between the velocity fields for the two fuels studied as well as for the previously measured ethene flame are presently being made. The results of these comparisons will determine the need for detailed velocity measurements in other flames to be studied.

4. A series of studies in the high pressure diffusion flame facility have been completed. In these experiments, ethene/air flames have been studied over a pressure range of one to four atmospheres. The results of these studies are being used to examine the pressure dependence of the soot formation process. These initial studies are being used as a comparison with previous work as well as to independently verify the relationship between operating pressure changes and soot formation processes.

5. During the course of the study of a series of high pressure methane diffusion flames, an interesting flame instability phenomena was observed. This phenomena occurred spontaneously as the pressure increased above approximately 1.5 atmospheres. No similar

instability had been observed for the ethene flames at these pressures. High speed video cinematography using a Spin Physics camera was used to reveal a very regular pulsating flame structure. A limited series of studies of these flames has been undertaken and will be described later in this report. These well controlled pulsating structures may provide a controlled systematic approach for studying soot formation in an unsteady flame environment.

6. Modeling efforts for both the laminar and pulsating flames have been initiated during the past year. Work using the model developed by Mitchell [7] has been the focus of most of the work. However, recently collaborative efforts with R. Davis of the National Institute of Standards and Technology and C. Merkle in the Mechanical Engineering Department of Penn State have shown potential for future work. These efforts will be briefly described at the end of this report.

4.1 Atmospheric Laminar Diffusion Flame Studies

One of the major elements of the present study is to quantitatively study the effect of fuel species on soot formation. However, a difficulty in studying fuel molecular structure effects lies in the wide differences in the flame size and shape which results when various fuels are burned at, for example, a characteristic condition such as the soot point. The resulting differences in the temperature and velocity fields make quantitative comparisons impossible between the flames [13].

In the present studies, this difficulty is addressed by adopting a fuel addition approach involving well characterized baseline flames in which the soot particle field is characterized in detail. The fuel molecular structure effects are then investigated by adding an additional fuel component to the baseline flame. However, the total carbon flow rate is kept constant. This means that an appropriate fraction of the baseline fuel is replaced by the added fuel species. With the soot contribution from the baseline fuel known, the effect of the added fuel on the formation of soot particles can be examined. Under these conditions, the flame size and shape remains similar for all flames.

Two fuels, methane and ethene, have been selected to serve as the baseline flames. The methane flames have relatively low soot particle formation and, thus, provide greater sensitivity for measuring changes introduced by varying the fuel molecular structure. The ethene flames represent the best studied set of diffusion flames presently available and provide a significant comparative data base. The results obtained in the ethene baseline flames for a number of fuel species were reported in last year's annual report. Since that time, studies involving the methane baseline flame have been emphasized.

A series of three flames in which butane, 1-butene and 1,3 butadiene were added to a methane flame have been investigated. The flow conditions for these flames are shown in Table 1. In addition to the flow rates, this table lists the conversion percentage and adiabatic flame temperature as calculated from the NASA Equilibrium code [14]. The conversion percentage tabulated is based on the amount of fuel species added to the flame which is converted to soot particles.

Table I
Flow conditions for the butane, butene, and butadiene addition studies

Baseline Fuel	Flow Rate (cm³/s)	Fuel Added	Flow Rate (cm³/s)	% Conversion*	T_{ad} (K)
CH_4	5.6	C_4H_{10}	1.05	12.2	2243
CH_4	5.6	C_4H_8	1.05	35.1	2259
CH_4	5.6	C_4H_6	1.05	44.4	2285

* $\rho = 1.8$ gm/cm³

The contribution of the baseline fuel is subtracted from the soot present in the flame based on the studies of the atmospheric baseline flames. The carbon conversion percentage is calculated for the axial location displaying the maximum value of F_v, the integrated soot volume fraction:

$$F_v = 2\pi \int_0^R f_v \ r \ dr \tag{9}$$

where R is the radius of the soot particle field. The carbon conversion percentage can be expressed as

$$\% \ conversion = \frac{m_s - m_{sB}}{m_c - m_B} \times 100 = \frac{m_s - m_{sB}}{m_{add}} \times 100 \tag{10}$$

where m_s is the soot mass flow rate at the location of maximum F_v for the flame containing the fuel addition, m_{sB} is the corresponding soot mass flow rate for the pure baseline flame, m_c is the mass flow rate of carbon entering the burner, m_B is the mass flow rate of carbon contained as baseline fuel and m_{add} is the mass flow rate of carbon corresponding to the fuel species added to the flame. The determination of the soot mass flow rate at a particular height in the flame can be calculated from:

$$m_s (z_m) = 2\pi\rho \int_0^R v(r, z_m) \ f_v(r, z_m) \ rdr \tag{11}$$

where z_m is the axial location where F_v is a maximum, ρ is the density of soot and v is the velocity. Thus, the velocity profile must be known to precisely calculate the value of m_s. For the present analysis, the velocity has been assumed to be independent of r with a value for axial location z_m taken from Ref. 15. This is a reasonable assumption for the locations for which F_v is observed to be a maximum [15]. With this assumption m_s can be expressed as

$$m_s (z_m) = \rho \ v(z_m) \ F_v(z_m) \tag{12}$$

where ρ is taken to be 1.8 g/cm³.

As previously reported for the ethene baseline flames [16], Table 1 shows that a significant amount of fuel carbon can be converted to soot particles under these conditions. This result has serious consequences for real combustor conditions where multicomponent fuels are typical. Under such circumstances a knowledge of the degree of carbon conversion is of value if effects of variations introduced through fuel composition changes are to be assessed.

In order to better understand the processes responsible for the variation in the amount of soot produced in these flames, two specific aspects of the problem have been examined. The first involves characterizing the preparticle and particle inception regions, while the second investigates the surface growth process. Information concerning the preparticle chemistry which leads to soot precursor species is difficult to obtain. In the present studies, laser fluorescence from large hydrocarbon species excited by visible light at 488 nm and monitored at 514.5 nm was used to characterize the species leading to soot particles [3,17-20]. Although the observed fluorescence has not been attributed to a single species or group of species, its observation is usually linked to the preparticle chemistry region.

4.1.1 Soot Particle Inception

For the present experiments, the same apparatus previously described for the soot particle measurements was also used for these fluorescence studies. The argon ion laser is tuned to the 488 nm laser line and the fluorescence signal is measured with the photomultiplier detector located at 90° to the incident beam. Detection of elastically scattered light from the soot particles in the laser beam was eliminated by using a combination of a polarizing filter and narrow band filter (centered at 514.5 nm) located in front of the photomultiplier. Accompanying the laser fluorescence measurements were a set of detailed measurements of the soot particle field in each flame. These two measurements allowed for a comparison between the observations for each of the fuels studied.

To illustrate the overall behavior in these flames, figures 2 and 3 show the integrated fluorescence and integrated soot volume fraction as a function of height in the flame. These measurements are obtained by integrating the fluorescence and soot volume fraction measurements along the radial coordinate at a particular axial location as given in equation 9. These quantities represent a measure of the total fluorescence and soot volume fraction observed at a particular height.

From these results it is clear that the fluorescence and soot volume fraction increase similarly as a fuel's propensity to soot increases. Additionally, the fluorescence signals are observed to precede the soot particle inception process and increase dramatically as the soot particles form and grow. Comparisons between the integrated fluorescence and soot volume fraction axial profiles indicate that between 25% and 35% of the soot growth occurs before the fluorescence signals are observed to achieve a maximum value.

The fact that fluorescing species continue to increase subsequent to soot particle formation has not been previously observed. This observation leads to the possibility that large hydrocarbon species may also contribute to the early surface growth process as well. Previous work on surface growth of soot particles has assumed acetylene is the major gas phase reactant participating in the growth mechanism [21,22]. Because of the importance of the available surface area to subsequent growth processes, the role of these large hydrocarbon species in the surface growth process has been explicitly considered.
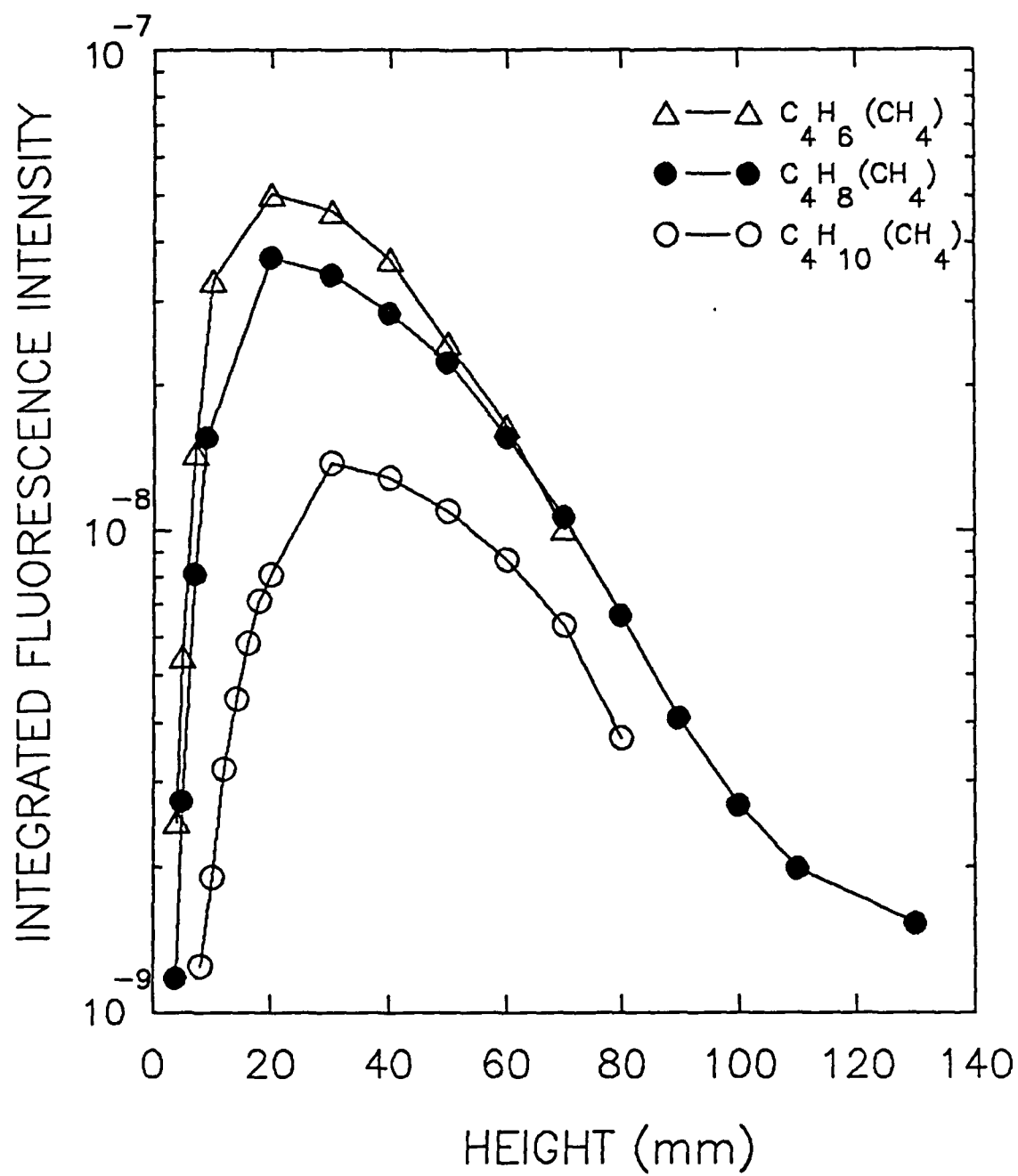
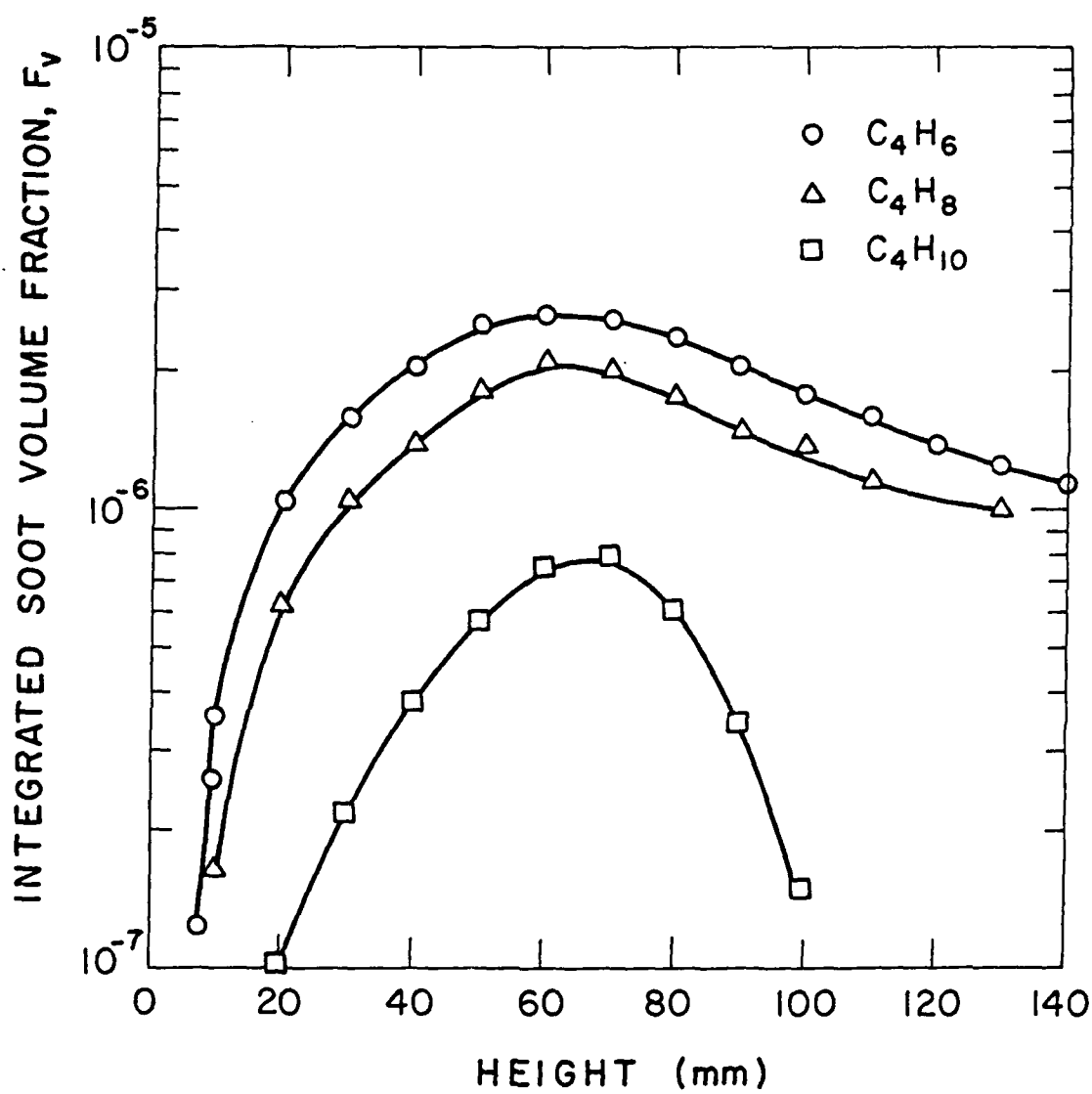Figure 2.   Fluorescence intensity integrated
over the flame diameter.

Figure 3. Soot volume fraction integrated over the flame diameter.

In order to further examine the relationship between the observed laser fluorescence and the formation of soot particles, comparisons between these fluorescence and soot volume fraction measurements along individual particle paths in the flame have been made. As previously described, this representation of the data is achieved using the velocity field measurements obtained in a similar ethene/air laminar diffusion flame. Because buoyancy dominates in these flames, the velocity fields do not strongly depend on the initial flow conditions over the range of conditions pertaining to these flames. Present studies are examining the accuracy to which this assumption holds.

Using this approach figures 4 and 5, show the comparison between the fluorescence and soot volume fraction measurements in two characteristic regions. Figure 4 displays the results along the particle path exhibiting the maximum soot volume fraction while figure 5 shows similar results along the centerline of the flame. In general, the observed trends are the same as in the integrated results displayed in figures 2 and 3. The fluorescence measurements are observed to precede the formation of soot particles and then to increase rapidly in the early formation period. Comparisons along individual particle paths indicate that between 20% and 70% of the soot growth occurs prior to the fluorescence achieving a maximum value depending on the particle path location in the flame. This point again raises the question as to the participation of large hydrocarbon species, which are responsible for the fluorescence observed, in the surface growth process. This point will be addressed below.

A few additional comments concerning the relationship between the maximum fluorescence observed and the onset of soot is warranted. Previously, it has been reported that at a particular height in the flame the region of maximum fluorescence coincides with the particle inception region [3,13]. In fact, this was observed to be true in both the annular and centerline regions. At first consideration, the present results appear to contradict these results. However, this contradiction can be resolved by realizing that the measurements shown in figures 4 and 5 are for a particular particle path and the fluorescence values do not necessarily correspond to the maximum fluorescence value at each height. A detailed review of the present results indicates that in the annular region, the maximum fluorescence location at a particular height still occurs where soot particles are first observed. Additionally, the maximum intensity increases with height while shifting in location towards the centerline.

Along the centerline, the first detectable soot particles are observed at the fluorescence maximum. Thus, most of the soot volume fraction increase occurs in the region following the maximum in fluorescence. This analysis is complicated by the fact that the minimum detectable soot volume fraction is about five to ten times smaller in the annular region of the flame. This is a result of the inversion of the line-of-sight extinction measurements to obtain local measurements of the soot volume fraction. For the present flame configuration, these measurements are least sensitive at the centerline for lower positions in the flame. This is largely a result of the fact that the majority of the extinction is due to the substantially larger amounts of soot found in the annulus of the flame at these heights. Thus, the actual particle inception region likely precedes the fluorescence maximum similar to that observed in the annular region.

The results described above lead to the following observations:

1. The species responsible for the observed fluorescence increase in proportion to the sooting tendency of the fuels studied. In this respect, such species satisfy one criteria for representing the soot precursors.

2. These fluorescing species precede the particle inception region throughout the flame zone. This is, of course, a minimal condition for a precursor species.

3. Following particle inception, these species increase rapidly during a significant fraction of the particle surface growth process. This leads to the possibility that such species contribute to the early surface growth process as well as the inception process.
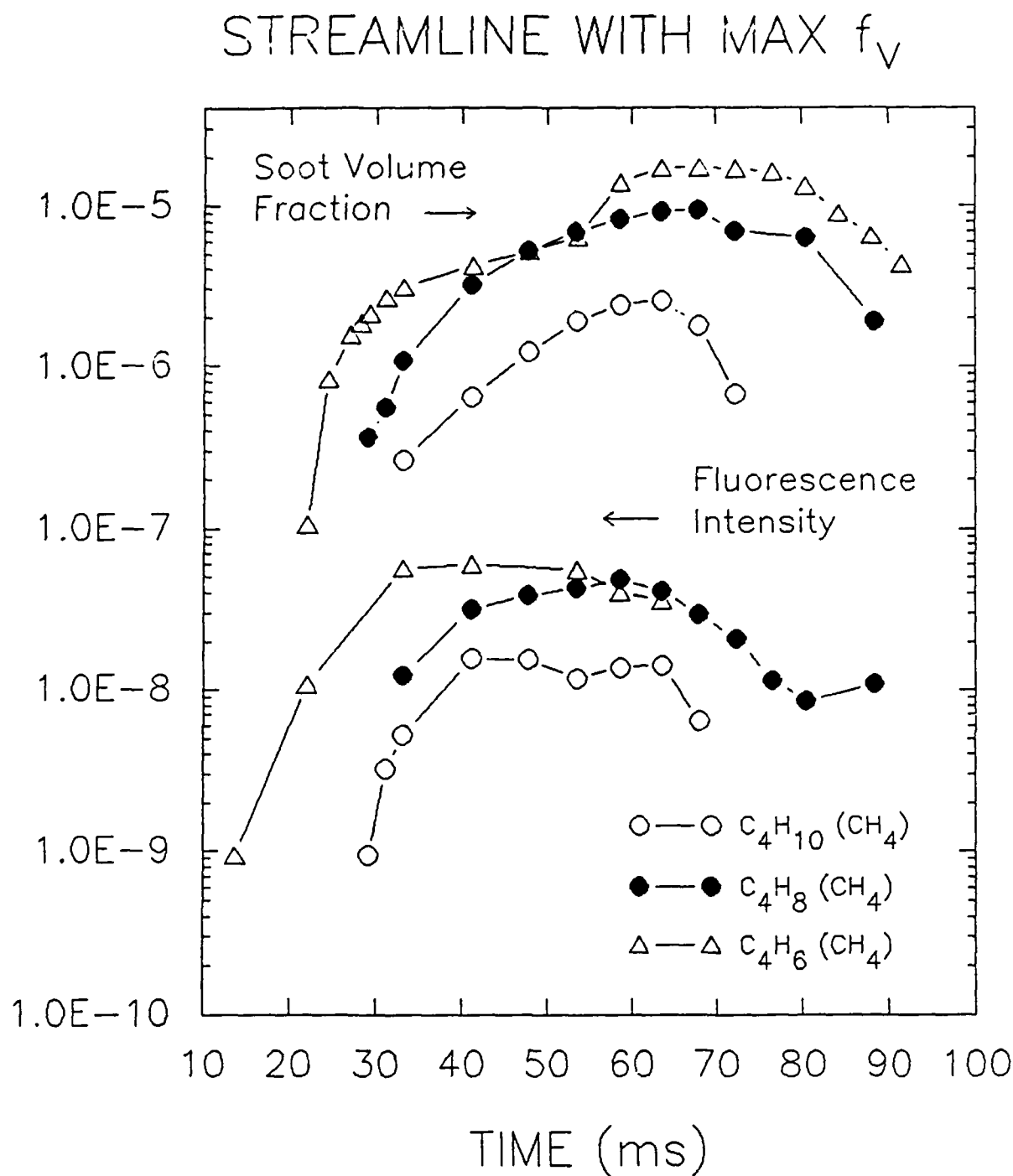
STREAMLINE WITH MAX f_V

Figure 4. The soot volume fraction and fluorescence
measurements along the particle paths of
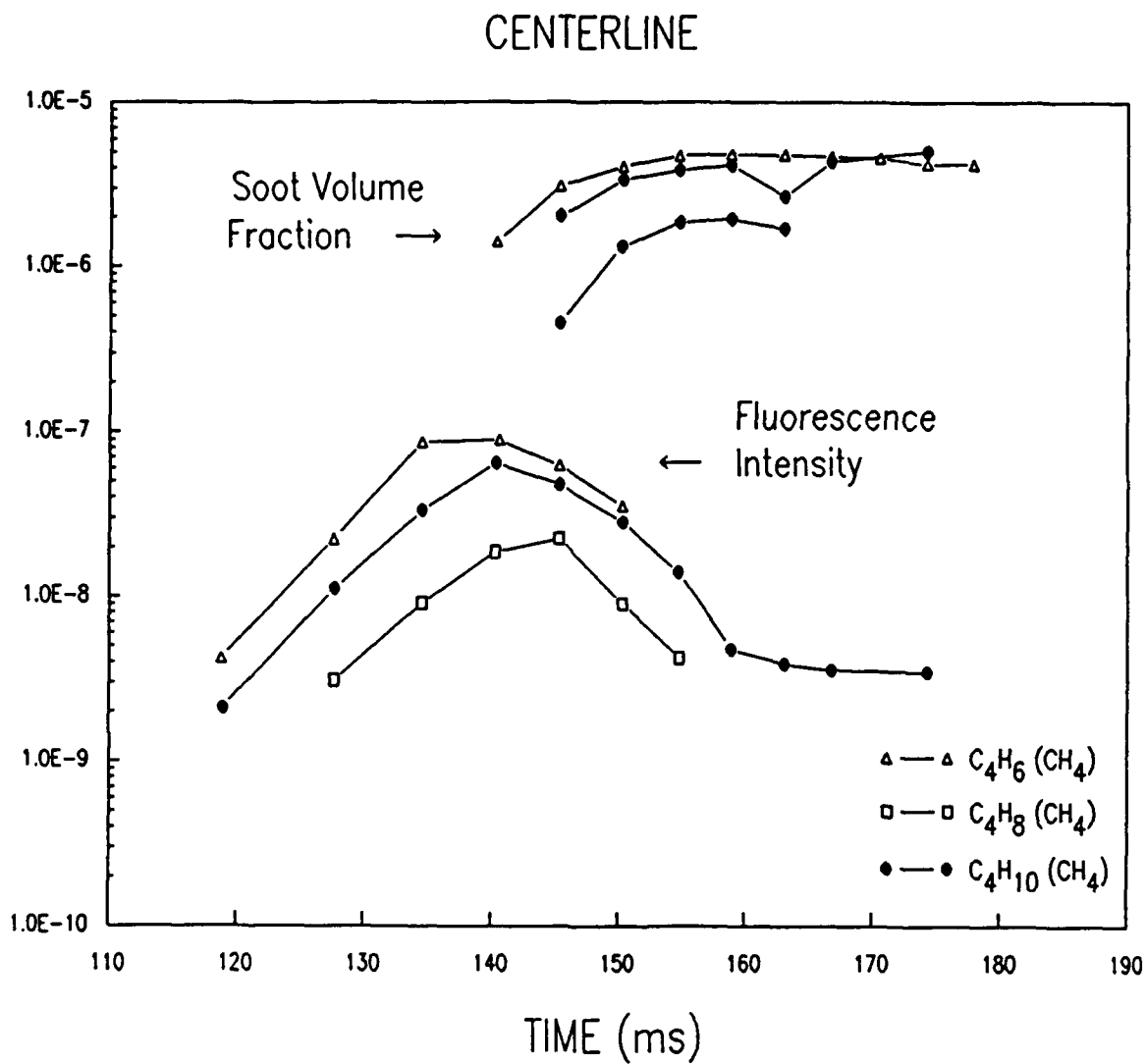maximum soot concentration in the annulus
region.

CENTERLINE

Figure 5. The soot volume fraction and fluorescence measurements along the centerline of the flame.

Although the above results provide additional insights into the early particle formation region, quantitative understanding has not been achieved. Several additional pieces of information would be of value. As with previous workers studying fluorescence from diffusion flames, no specific species identification or concentration levels have been quantitatively obtained. However, the potential for a qualitative chemical kinetic model comparison has been initiated. If the fluorescence is identified as a broad marker for large polycyclic aromatic hydrocarbons (PAH), the relative temporal and fuel dependent behavior observed in these flames can be compared with present soot kinetics models [23]. In such a comparison, only relative trends could be examined. However, such an approach might lead to general insights valuable for model development as well as for guiding future experiments. Before such comparisons can be attempted, temperature measurements in these flames must first be obtained. These experiments are planned as part of the present effort.

A second area for further work involves obtaining more quantitative information regarding the soot precursors. Two approaches to this problem are being planned. One involves an optical absorption study, while the second employs mass spectrometric sampling of gases from the flame. These aspects of the research program will be addressed at the end of this report.

4.1.2 Soot Particle Surface Growth

As was previously mentioned, these atmospheric flame studies are intended to investigate the particle inception and surface growth processes as a function of fuel structure. Clearly the results described above for the particle inception region show a strong sensitivity to the fuel under study. Thus, it is equally interesting to determine the effect of fuel molecular structure on the surface growth process for soot particles formed in diffusion flames. An additional point of interest lies in the role that large hydrocarbon species may have in the early surface growth process. This aspect arises from the results described above, in which the fluorescence signals attributed to large PAH species maximized at some significant fraction of the mass addition to the soot particles. Thus, allowing the possibility that these species contribute significantly to early soot growth.

In order to examine these two questions, the soot particle growth rate has been examined in the previously described butane, 1-butene and 1,3 butadiene addition studies. The analysis has been carried out along the same two particle paths for which measurements are shown in figures 4 and 5. Thus, the results to be discussed typify both the annular and center regions of these flames. The present approach to the analysis is to represent the soot mass growth rate as

$$\frac{dm}{dt} = k \, S \, [C_x H_y] \qquad (13)$$

where m is the mass of soot (g/cm^3), k is the surface growth rate constant (g/cm^2-s-atm), S is the specific surface area (cm^2/cm^3) and [C$_x$ H$_y$] is the species concentration reacting with the surface to add mass [atm]. In the present experiments the product of k and [C$_x$ H$_y$] can be determined since S and dm/dt can be determined from the combined light scattering and velocity measurements. This product, k [C$_x$ H$_y$], is termed the specific surface growth rate constant. The specific surface area is calculated from the particle diameter and number density measurements while the soot mass growth rate can be found from the measured soot volume fraction assuming the density of soot particles is 1.8 g/cm^3. In last years annual report, the specific surface area was shown to be a strong function of fuel structure for a series of fuel addition studies to an ethene baseline flame. In that case, the fuels studied included ethene, propene, 1-butene and toluene. The present studies for butane, 1-butene and 1-3 butadiene represent a more systematic variation of chemical bonds and conjugation as well as a variation in the baseline flame (methane vs. ethene). Nonetheless, the results are similar to those for the ethene flames. Figures 6 and 7 show the specific surface growth rate constant for the present C$_4$ fuel studies in the annulus and along the centerline. As with the previous ethene/fuel addition studies, the behavior for each fuel is similar. Shortly after the particles are formed, the specific surface growth rate is close to 2×10^{-4} g/cm^2-s. After a period for which this rate constant is approximately constant, the surface growth rate drops rapidly. It should be pointed out that the present analysis has been limited to the region of the flame before the soot volume fraction reaches a maximum. Thus, regions where soot particle oxidation dominates have been excluded from consideration.
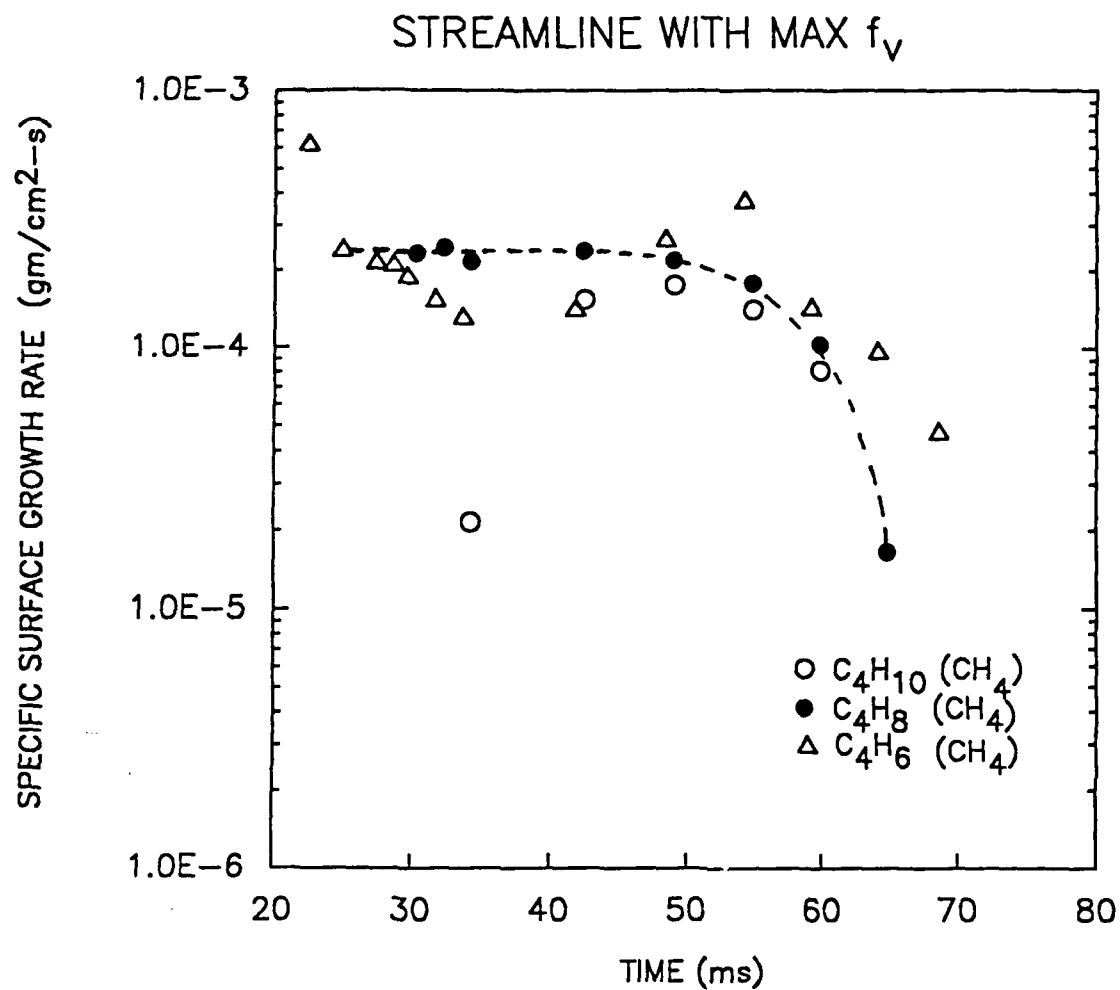
Figure 6. The specific surface growth rate vs. time for the butane, 1-butene and 1,3 butadiene addition studies to the methane baseline flame. Results along the particle path containing the maximum value for the soot volume fraction.
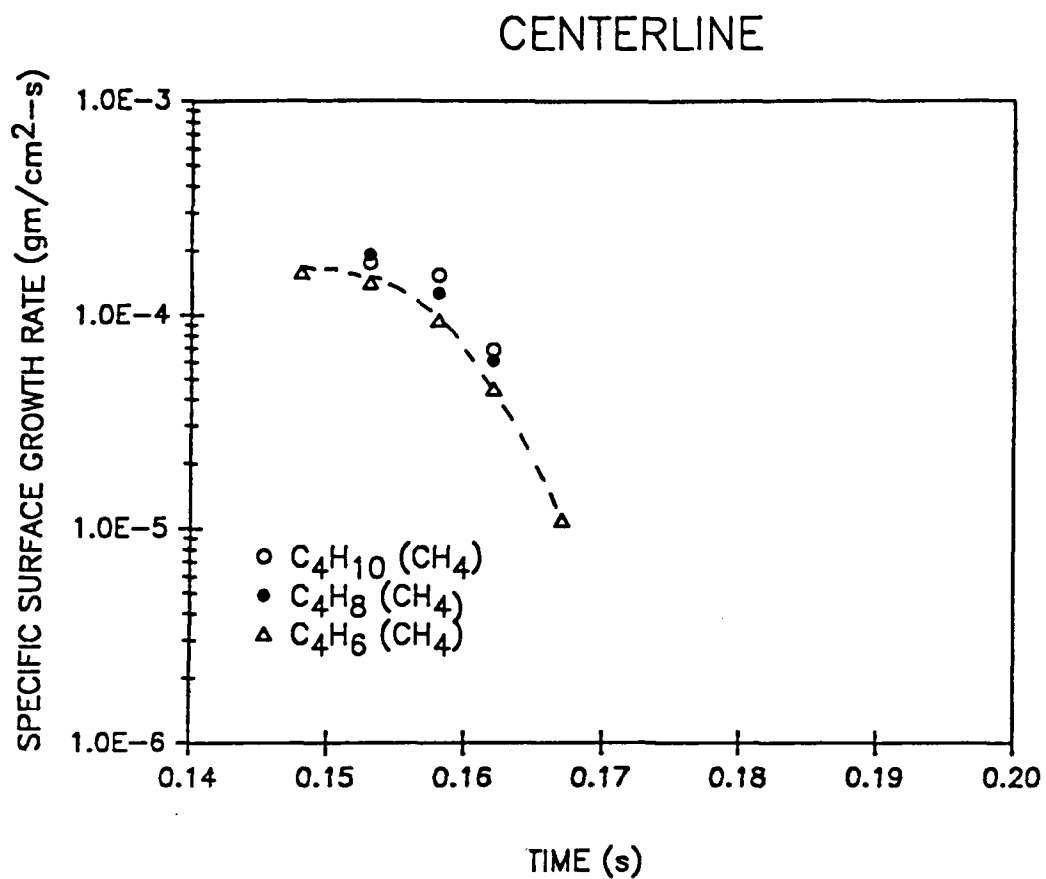
CENTERLINE

Figure 7. The specific surface growth rate vs. time for the butane, 1-butene and 1-3 butadiene addition studies to the methane baseline flame. Results along the centerline of the flame.

Figure 8 shows the results for the ethene baseline flame studies where ethene, propene, butene and toluene were added to the flame. Clearly the same general behavior is observed in these flames. Also shown in figure 8 are the results of a rich ethene/air premixed flame studied by Harris and co-workers [21,22]. It is interesting to note that although the temporal behavior of the specific surface growth rate differs, there is order of magnitude agreement between the value for this rate constant in both flame systems.

From these extensive studies, it is clear that the surface growth process is similar in all the flames studied here. Furthermore, since accounting for the differences in available surface area substantially explains differences in the growth processes for flames of widely differing soot concentrations, the value of the initial surface area is critical to subsequent surface growth. Additionally, these studies show that similar values of specific surface growth rate are found throughout the flame for the fuels studied.

Before making further observations concerning the present status of understanding in the area of soot particle surface growth, some discussion of the effect of the fluorescing species in this process is appropriate. Clearly, if the initial surface area is important in all subsequent growth, species involved in the first stages of surface addition should be carefully examined. The results described in the soot particle inception section of this report (4.1.1) showed that the fluorescence measurements attained a maximum after some significant fraction of the mass contributed by surface growth had occurred. To quantify the contribution of large hydrocarbon species attributed as the source of the observed fluorescence, a series of highly spatially resolved radial profiles of the soot particle field were obtained for closely spaced intervals along the axis of the flame. These profiles correspond to the earliest data points shown in figure 6. With the exception of the butadiene flame, no systematic increase in the specific surface growth rate constant is observed. Thus, the present data does not support a model in which the species observed in the fluorescence measurements contribute extensively to the surface growth in the region immediately following particle inception. These species may contribute to the particle inception process.

The experiments described in the last two sections have identified some key questions for consideration. The surface growth process has been shown to be similar for a variety of fuel structures and sensitive to the initial surface area available for growth. Thus, it now is clear that a quantitative understanding of the relationship between the soot precursors and this initial surface area is required for a more complete description of soot formation in combustion systems. The present approach of concentrating on the initial particle inception region is sound, but it needs to be expanded in terms of diagnostic approaches and quantities measured. Present directions include applying optical absorption and mass spectrometric measurement techniques to these flames.

In addition, there is a need to ascertain specifically the growth species involved in the surface growth process. This should be possible using similar mass spectrometric measurements in the particle growth region. These measurements require developing probe sampling techniques capable of sampling gases in soot particle laden regions without plugging the probe. Recent studies in our laboratory using charged probes similar to those developed by Sangiovanni [24] have shown some promise in this respect for regions above the flame. These approaches need to be refined and extended to lower portions of the flame.

Finally, the causes for the decrease in the specific surface growth rate constant need to be resolved. Both reductions in particle surface reactivity and increased competition from oxidation processes are plausible explanations. However, there is a need to resolve which mechanism is actually controlling and under what conditions it dominates, if quantitative predictions are to result.

The specificity and limited number of these questions is an indication of the progress achieved in the study of surface growth processes related to soot formation. Clearly a general, quantitative picture of this portion of the soot formation process is emerging. There is a need to achieve a similar level of understanding to the particle inception and oxidation regions of the process.
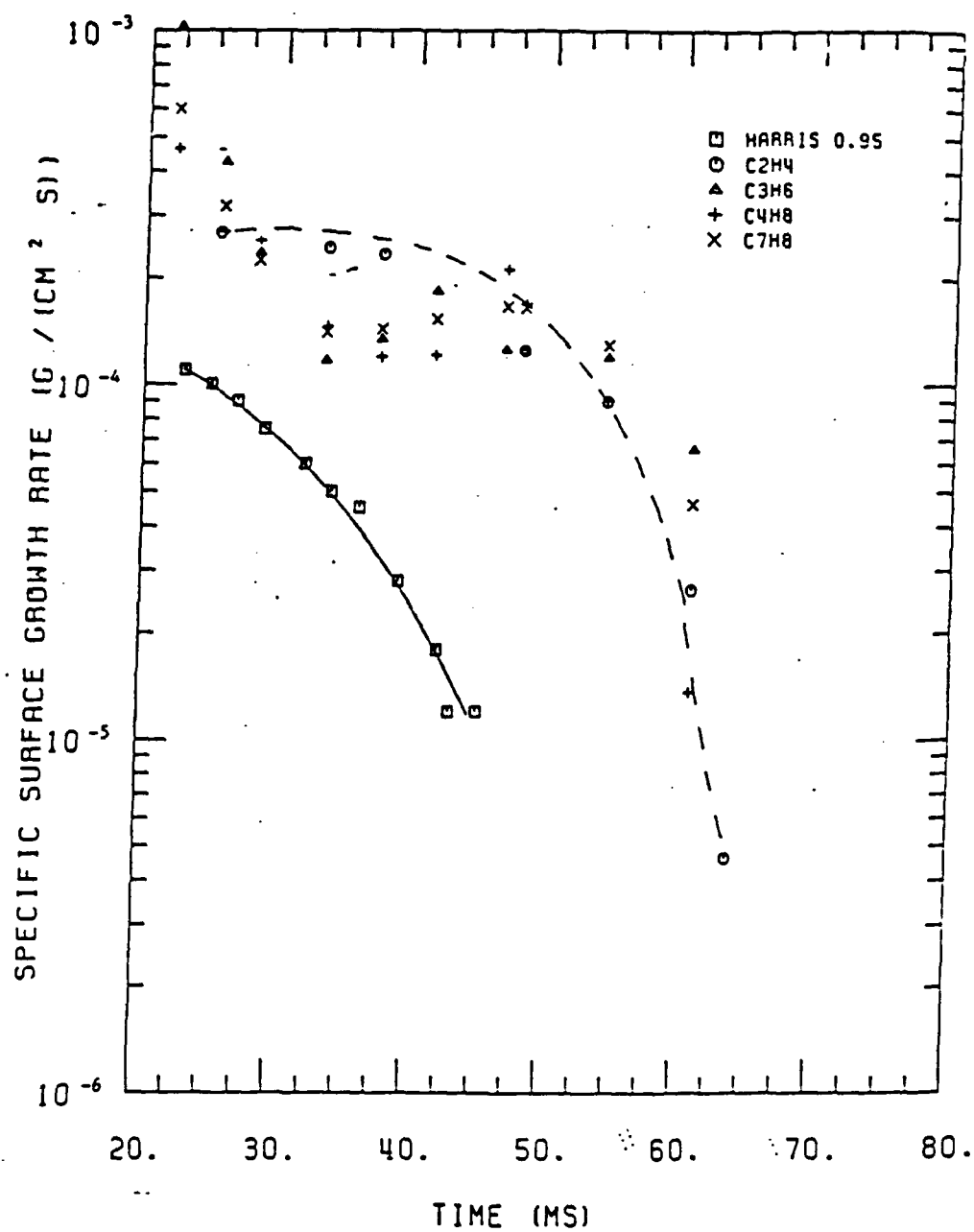
Figure 8

Specific surface growth rate along the particle path exhibiting the
maximum soot volume fraction. The dashed line (---) is a best faired
curve through the ethene flame results.

4.1.3 Velocity Field Measurements

In the present studies, information on the temporal evolution of the soot formation processes is obtained by combining measurements of the velocity and soot particle fields. Detailed measurements of the velocity field provide the basis for identifying individual particle paths and, thus, to follow particle inception, growth and oxidation. In the results described previously in this report, the velocity field measurements have been taken from studies of ethene/air flames under very similar flow conditions [15]. These studies have established that the velocity field is dominated by buoyancy and is not strongly sensitive to the initial flow conditions for the range of conditions employed in the present studies. However, direct experimental evidence of the accuracy of this approach is desirable. To this end, a series of velocity measurements in the butane/methane and 1-butene/methane flames previously described (see Table 1) have been completed.

These measurements were obtained using a laser velocimetry technique capable of determining a single velocity component. Both axial and radial components of the velocity were obtained separately. The highly stable nature of the present laminar flame system eases the requirement for simultaneous measurement of the velocity components. Figures 9 and 10 show a comparison of the results for these experiments for both the axial and radial components. There is clearly a strong similarity in the profiles of the two flames as well as with previously published results for the ethene/air laminar diffusion flames [15]. Presently, analysis is concentrating on determining the sensitivity of the surface growth analysis to the velocity field utilized to construct the particle paths.

One of the objectives of the present analysis is to establish the limits over which a single velocity field determination can be used to analyze a series of fuel mixture studies. This allows an evaluation of the approach of using a baseline flame as equivalent to a flow reactor in which different fuels are introduced. Since the conditions in the baseline flame are only perturbed slightly, this approach represents a powerful and well controlled approach to study soot formation for a variety of fuels. The ability to use a single velocity field to approximately represent the flow field in all of the fuel addition studies, represents a major experimental simplification in terms of measurement requirements for each fuel studied. The present data will allow a direct quantitative evaluation of the appropriateness of this approach for treating the velocity field.

4.2 High Pressure Diffusion Flame Results

Studies of the effect of pressure on soot formation under diffusion flame conditions have been quite limited. Recently, Flower and coworkers have undertaken to examine the effect of pressure for a series of ethene/air flames [25-27]. Their results have been extremely interesting, leading to new insights into the question of soot formation at high pressures. Although these previous studies were well done and extensive, a number of questions remain to be examined. The present experiments investigating laminar diffusion flames operating at high pressures are intended to directly introduce the effects of fuel structure as well as clarify in more detail processes contributing to the increases in soot formation observed (for example, effects on particle size and number concentration).

During the past year, efforts have concentrated on obtaining results on a series of ethene flames over a pressure range of 1 to 4 atmospheres as well as to extend the experiments to other fuels. In the next two sections, the progress and problems encountered in achieving these objectives will be summarized.

4.2.1. Laminar Diffusion Flames Studies Under High Pressure Conditions

The assembly of the High Pressure Diffusion Flame Facility was complete near the end of the first year of the program. The details regarding this apparatus were summarized earlier in this report (see section 3.2). For the initial studies in this facility, an ethene/air diffusion flame was selected for investigation. This flame system has been extensively studied in this laboratory under atmospheric conditions. Additionally, Flower and coworkers have conducted studies at elevated pressures as well [25-27]. Thus, an extensive data base exists for comparison and validation of the
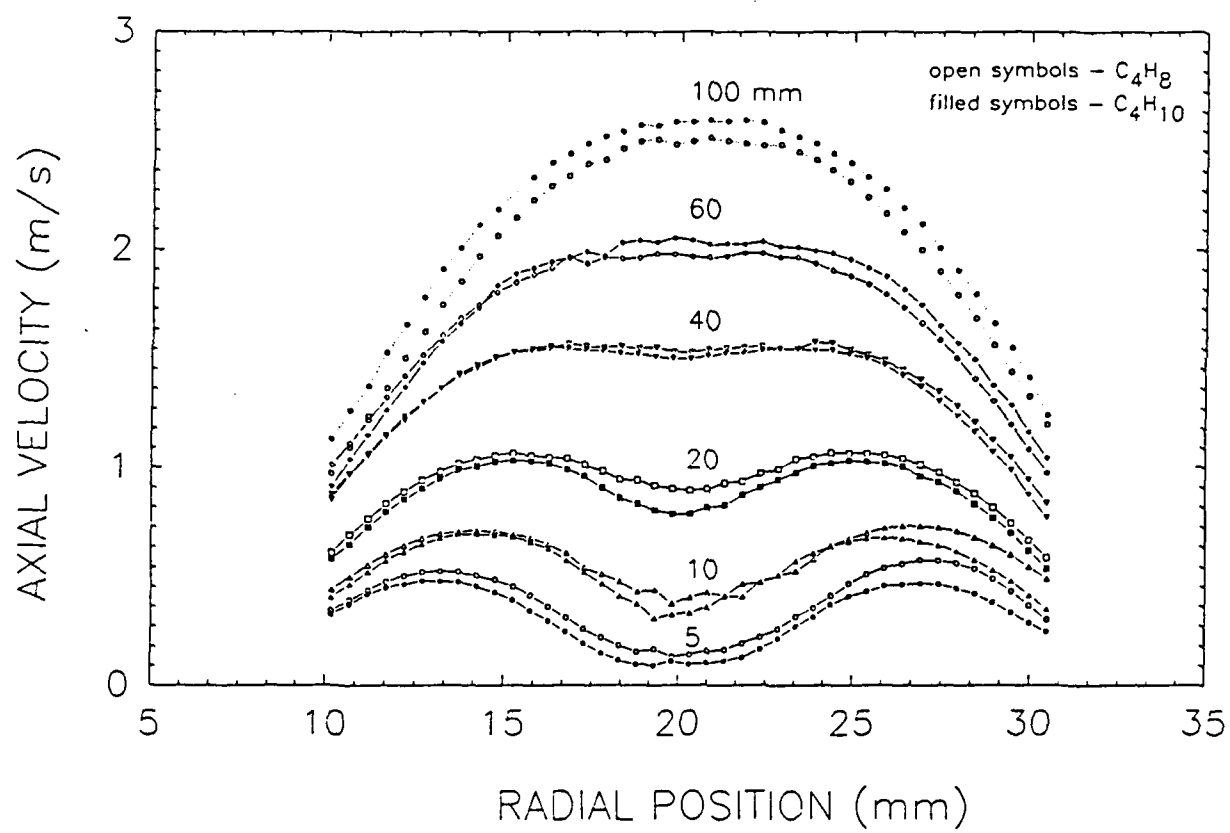
Figure 9. The axial velocity profiles for the butane and
1-butene flames as a function of radial position
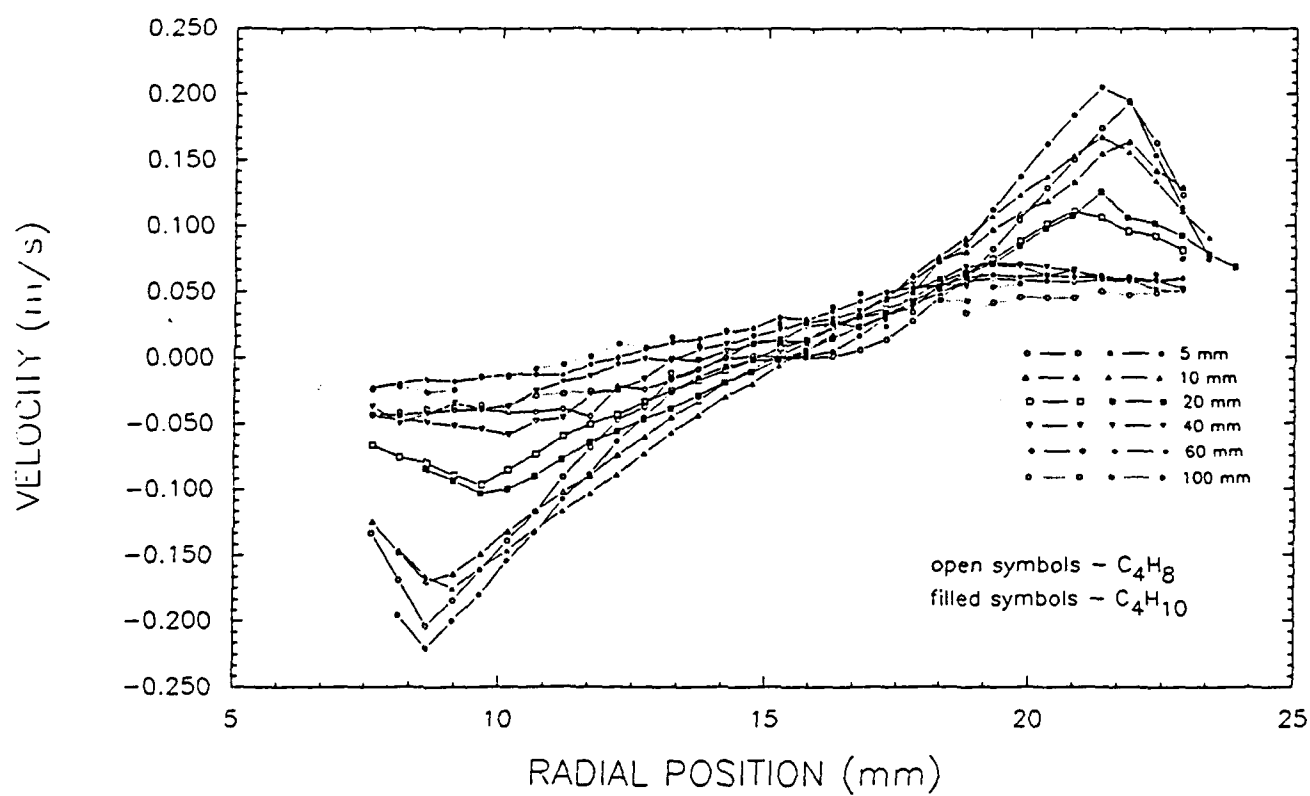for several axial positions in the flame.

Figure 10. The radial velocity profiles for the butane and 1-butene flames as a function of radial position for several axial positions.

operation of the present facility.

Before describing the results of these experiments, a brief summary of some of the difficulties encountered in the high pressure studies will be given. In the initial high pressure flame studies, several problems not encountered in previous atmospheric pressure experiments were observed. Two of these problems were directly related to the introduction of windows into the test cell. Studies done at atmospheric pressure simply used slots machined in the chimney of the burner to provide for optical access. The windows introduced multiple reflections of the incident laser beam and a significant increase in the background scattered light component due to inhomogeneities in the window material. These effects resulted in spurious intensity peaks in the scattered light profiles and a broadening of the gradient of these profiles due to the large scattered light component surrounding the main portion of the incident laser beam. Both of these effects were reduced to an acceptable level by the use of windows having appropriate anti-reflective coating as well as by selecting a quartz material having improved homogeneity. In this process, the window supplier, ESCO Products, was extremely helpful in supplying a variety of window sets for testing.

The second experimental difficulty did not involve the studies of the ethene/air flame system, but rather studies involving other fuel species. Specifically, the intended procedure for these high pressure studies was to involve a methane baseline flame using the fuel addition approach previously described. Methane was chosen because of its low propensity for soot particle formation, thus allowing for a sensitive study of fuel molecular structure effects as a function of pressure. The methane baseline flame selected for study had a flow rate of 9.8 cm^3/s and was quite stable at atmospheric conditions. However, as the pressure in the test chamber was increased to above 6 psig, a regular flame oscillation or pulsation was observed which continued as the pressure increased. No similar behavior had been observed in the ethene studies for which the fuel flow rate was 3.9 cm^3/s. In the next section, a more detailed discussion of this phenomena will be presented.

During the past year, some effort has been given to understanding and defining the flow regime over which stable flames can be achieved. Both studies of methane and ethane baseline flames have been completed and a suitable region for study has been identified. Ethane is also a fuel which has a low propensity for soot particle formation as compared to alkene, alkyne or aromatic fuels. At the present time, a series of studies using ethane as the baseline flame with propane and propene added to this flame over a pressure range of 1 to 5 atmospheres are planned. These experiments are intended as the first in a series to examine effects of fuel molecular structure on soot formation at elevated pressure.

The occurrence of the above difficulties further emphasized the need for the ethene/air studies as a comparative study. The ethene/air diffusion flames were studied over a pressure range of 1 to 4 atmospheres. Typical radial profile measurements for the light scattering and transmittance are shown in figures 11 and 12 for an operating pressure of 4 atmospheres. These measurements were obtained at 2.5 mm and 10 mm above the exit of the fuel tube for a flame whose ethene fuel flow rate was 3.9 cm^3/s. Several features of these measurements are of note:

1. The results, similar to previous atmospheric studies, generally exhibit excellent symmetry in the measurement profiles. This feature allows for application of tomographic inversion of the line-of-sight transmittance measurements to yield a local extinction coefficient. From the extinction determination, a direct measurement of the soot volume fraction is obtained.
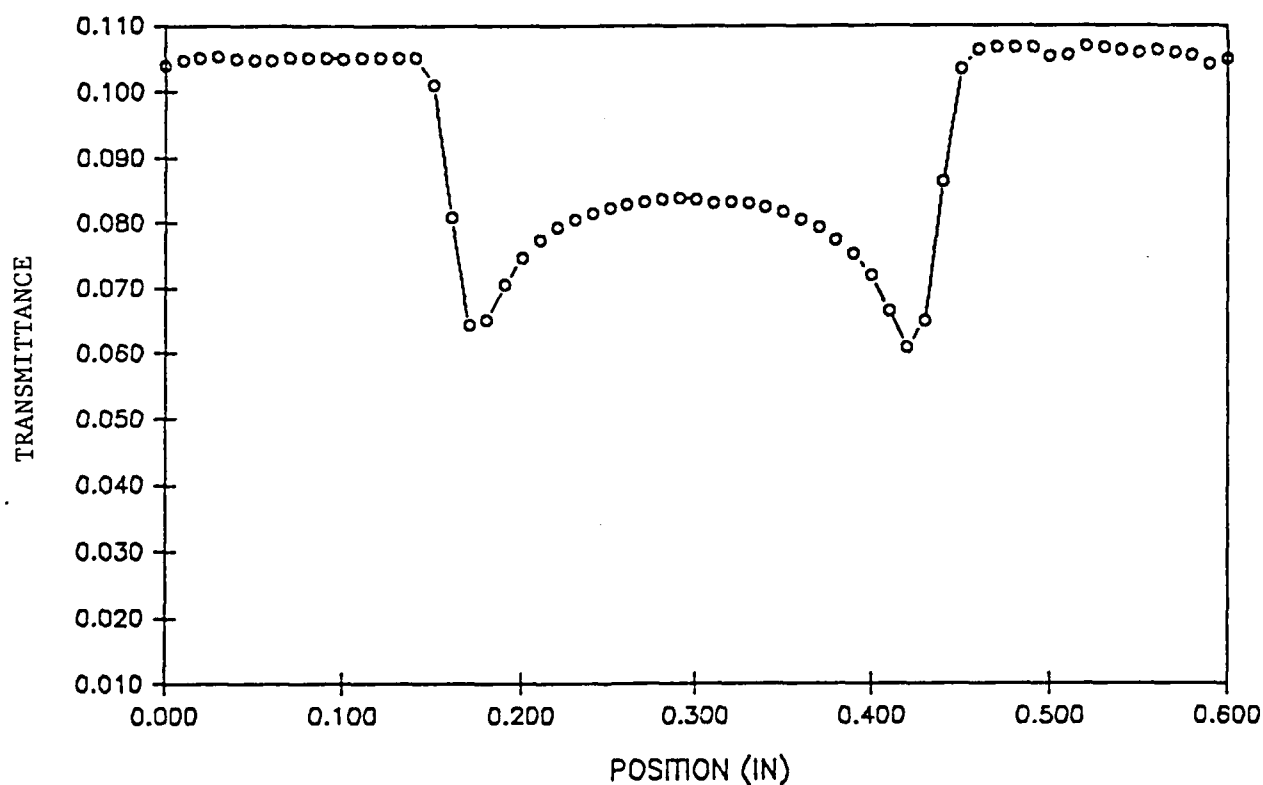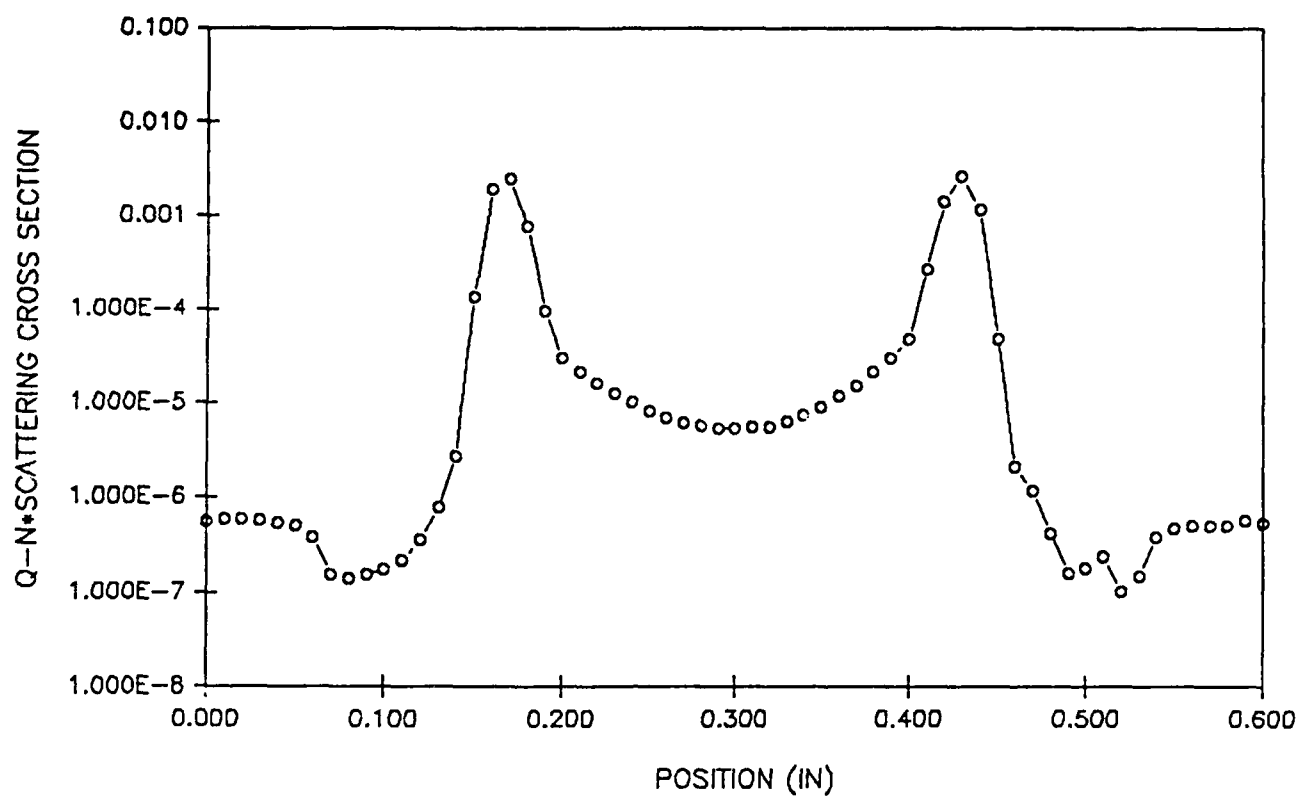
Figure 11.   The measured scattering cross section and transmittance
in an ethene/air diffusion flame at four atmospheres
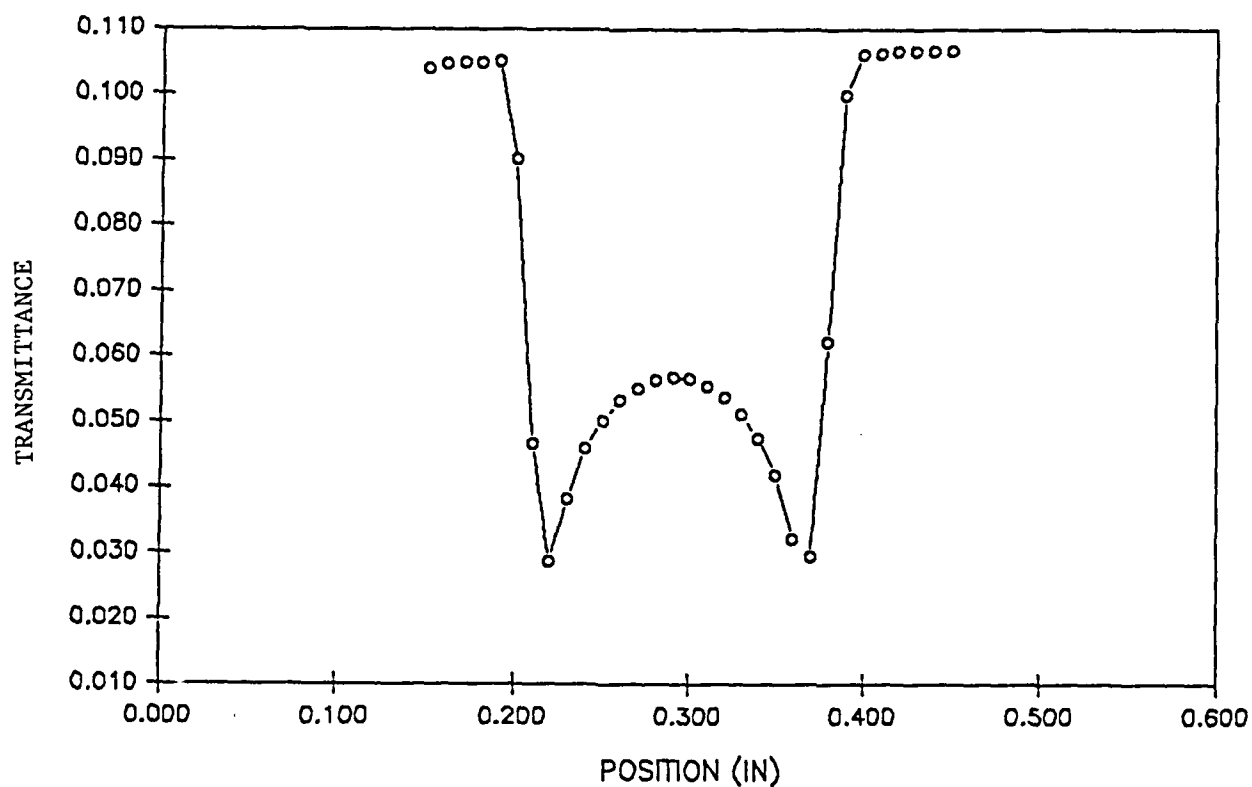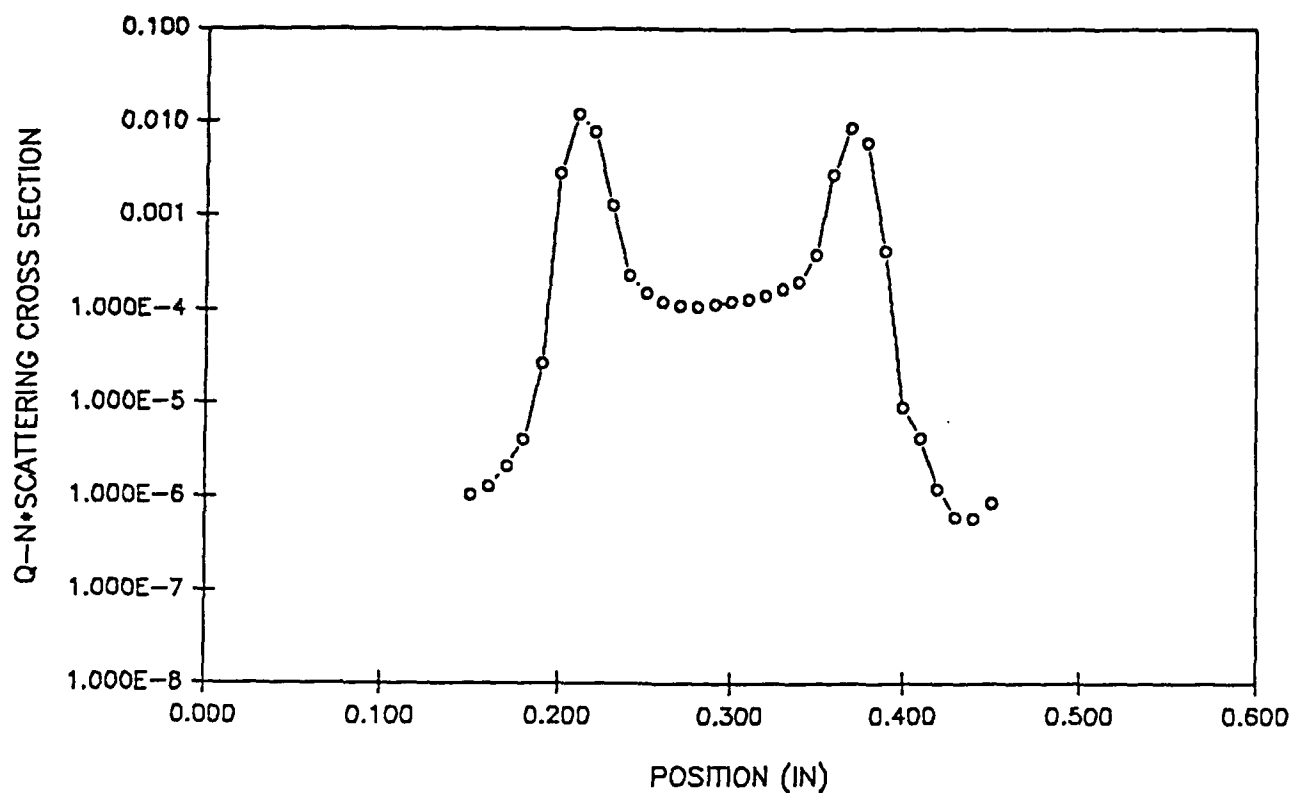pressure at an axial location 2.5 mm above the burner.

Figure 12. The measured scattering cross section and transmittance
in an ethene/air diffusion flame at four atmospheres
pressure at an axial location 10 mm above the burner.

2. Even at the lower axial position, significant light extinction is occurring indicating rapid formation of the soot particles in these flames. In fact, by the 40 mm axial position, nearly 80% of the laser beam is observed to be extincted in passing through the flame. This very strong absorption by the particles further illustrates the utility of the baseline flame approach for the study of highly sooting fuel components. As a point of comparison, at 2.5 mm in an atmospheric ethene/air diffusion flame, no measurable extinction would be observed.

3. Data analysis of these flames to yield volume fraction, particle diameter and number concentration are in agreement with the results of Flower [27]. Analysis of the 3 and 4 atmosphere flames yield an exponent of 1.12 for the pressure dependency (P^n) in agreement with that determined by Flower of 1.2 ± 0.1. These measurements are the first independent verification of these results.

Present plans call for additional analysis of these flames as well as to conduct experiments at 10 atmospheres. Of particular interest is to examine the onset and growth of the gas phase absorption reported by Flower for his highest pressure flames [27]. In light of the previous fluorescence studies conducted in this laboratory for atmospheric flames, these measurements are of particular interest in terms of soot particle precursor formation.

Concurrently, plans for the fuel molecular structure studies involving propane and propene in an ethane baseline flame are proceeding. These experiments are viewed as critical, since the previous studies by Flower had been limited to ethene flames. There is a significant need to establish whether the observed pressure dependence is similar for a variety of fuel species and to examine in more detail which aspects of the soot formation process are most strongly affected, i.e. particle inception or surface growth. In particular, it would be of interest to ascertain whether the surface growth process is strongly affected by pressure. It is possible that, similar to the atmospheric flame results, initial surface area following particle inception accounts for differences in the final amount of soot observed in these flames.

These studies are intended to be a focus of the efforts during the next year of the program.

4.2.2 Flame Instability Studies

In the course of the high pressure soot formation studies, an interesting flame instability problem was encountered. This problem was first observed for methane/air diffusion flames as the pressure was raised above one atmosphere. At approximately 6 psig (20.7 psia) the flame began to oscillate or pulsate. Ethene/air flames operated at pressures up to 4 atmospheres had not been observed to exhibit similar behavior. In order to examine this phenomena further, a series of high speed video images of this methane flame were recorded with a Spin Physics camera. These images were obtained at a framing rate of 500 frames per second and simply recorded the flame luminosity from the soot present in the flame. The replay of these video recordings at slower speeds revealed the onset and evolution of a very regular flame structure with a repetition rate of approximately 15 Hz. Similar phenomena had been described and analyzed in the literature under atmospheric flame conditions [28-30] or studied under acoustically forced conditions [31]. However, the observation of a clear pressure induced transition appears to be new and to offer the potential for new studies.

Figure 13 shows a series of selected images from the high speed video movie illustrating the evolution of the flame luminosity in these methane diffusion flames. The images shown in figure 13 are not consecutive frames, but were merely chosen to illustrate the general behavior of the flame. The image is recorded through the two inch diameter window of the high pressure diffusion flame facility and, thus, only a portion of the flame is shown. In the sequence shown (a-d), the flame gradually necks in and separates with the remaining section convected along the axis of the flame. This process repeats periodically at a constant frequency. Increasing the pressure causes the location of the necking region to move closer to the burner exit, while maintaining approximately the same frequency. In addition to affecting the location of the necking (referred to as tip cutting), the rate at which the separated portion of the flame is observed to disappear (that is oxidized) increases. This is presumably due to increased oxidation of the soot particles, which may be due to enhanced mixing or changes in temperature field.
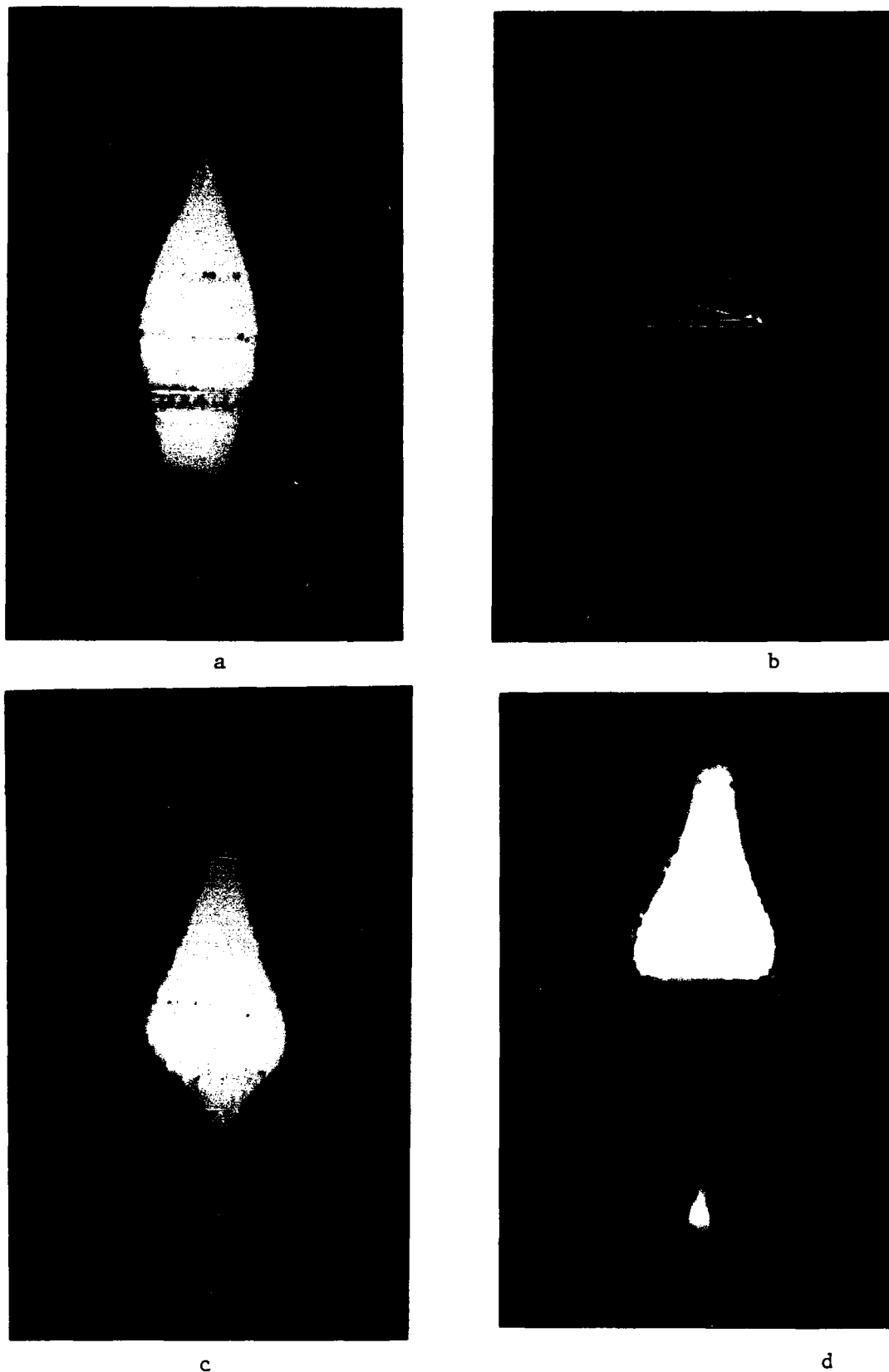
Figure 13. A selected sequence of high speed video images of the soot luminosity in a methane/air flame at 2 atmospheres pressure. a) intact flame, b) narrowed flame, c) near tip cutting flame, d) separated flame. Field of view approximately two inches

Several attempts were made to eliminate these pulsating flames by modifying the pressure chamber with baffles or screens. These changes were intended to alter the acoustic modes of the chamber or to impede flow recirculation. None of these approaches significantly affected the phenomena. Thus, the observed oscillations are believed to be self excited.

In addition to the high speed video recordings, a simple series of two-dimensional sheet visualizations were obtained using the 532 nm laser line from a Nd-Yag pulsed laser. In these images of light scattered from soot particles present in the flame were recorded on a two-dimensional array camera located at 90 degrees to the incident laser sheet. A series of these images is shown in figure 14. The earliest time corresponds to the upper left-hand corner of the figure with time increasing as one moves from left to right and downward. Clearly, the same process illustrated in Figure 13 is evident in this figure as well. In the two-dimensional imaging case, the well known spatial structure of the soot field is evident with the soot concentration highest near the outer annular regions of the flame. The progression shown in figures 13 and 14 is very regular and is strongly influenced by the pressure. Of additional interest is the rapid burnout of soot particles shown in the last two frames of figure 14 which may be a result of enhanced mixing. The observed process does not appear to be symmetric in the present case. The reason for this lack of symmetry is not understood at the present time.

Although this phenomena is dramatic in its nature, its importance in terms of providing further insight into unsteady combustion processes was not immediately evident. Shortly after the initial observations of this flame instability process, discussions with Dr. R. Davis of NIST raised several interesting possibilities concerning these flames. Dr. Davis has developed a theoretical model for unsteady buoyancy-driven jet diffusion flames. In the formulation of this model, three dimensionless parameters enter into the formulation: the Reynolds number, the Peclet number and the Richardson number. In the present experiments, because the mass flow rates of fuel and oxidizer are maintained at a constant value, the product of the density and inlet gas velocity remains constant as pressure is changed. Since the viscosity is independent of the pressure, the Reynolds number also remains constant as the pressure is varied. In the limit of unity Lewis number, the Peclet number is equal to the fuel jet radius multiplied by the ratio of inlet gas velocity and the binary diffusion coefficient of the fuel. Since both the inlet gas velocity and the diffusion coefficient are inversely proportional to the pressure, the Peclet number also remains constant.

Finally, the Richardson number, which expresses the ratio of buoyancy forces to inertial forces, can be expressed as gL/U^2 where g is the gravitational constant, L is the fuel jet radius and U is taken as the air inlet velocity. Clearly, this number will vary with the square of the pressure through the velocity term in this ratio. Thus, the _effective_ gravitational acceleration will vary as the pressure squared. Consequently, in Dr. Davis's model, a pressure of two atmospheres can be simply simulated by choosing a gravitational constant of 4 g.

The significance of the present experimental configuration is that relative effects of buoyancy can be examined in isolation from the other parameters. This situation is unique to this burner configuration and offers an excellent opportunity for investigating the fundamental aspects of the instability onset from both experimental and theoretical modeling aspects.

To date, Dr. Davis has performed some preliminary model comparisons with the imaging results described above. The agreement on the general features of these flame instabilities is quite good. The model accurately predicts the instability frequency and tip cutting location quite well. This agreement includes the prediction of the observation that the tip cutting location decreases as the pressure increases. One area where agreement has not been obtained to date, involves the pressure at which the onset of the instability is observed. The model predicts a pressure of about one half that observed experimentally.

Presently a brief article is in preparation describing these results. Future work could involve a more extensive measurement program on these flames which could include velocity, species concentration (such as OH) and soot particle concentration measurements.
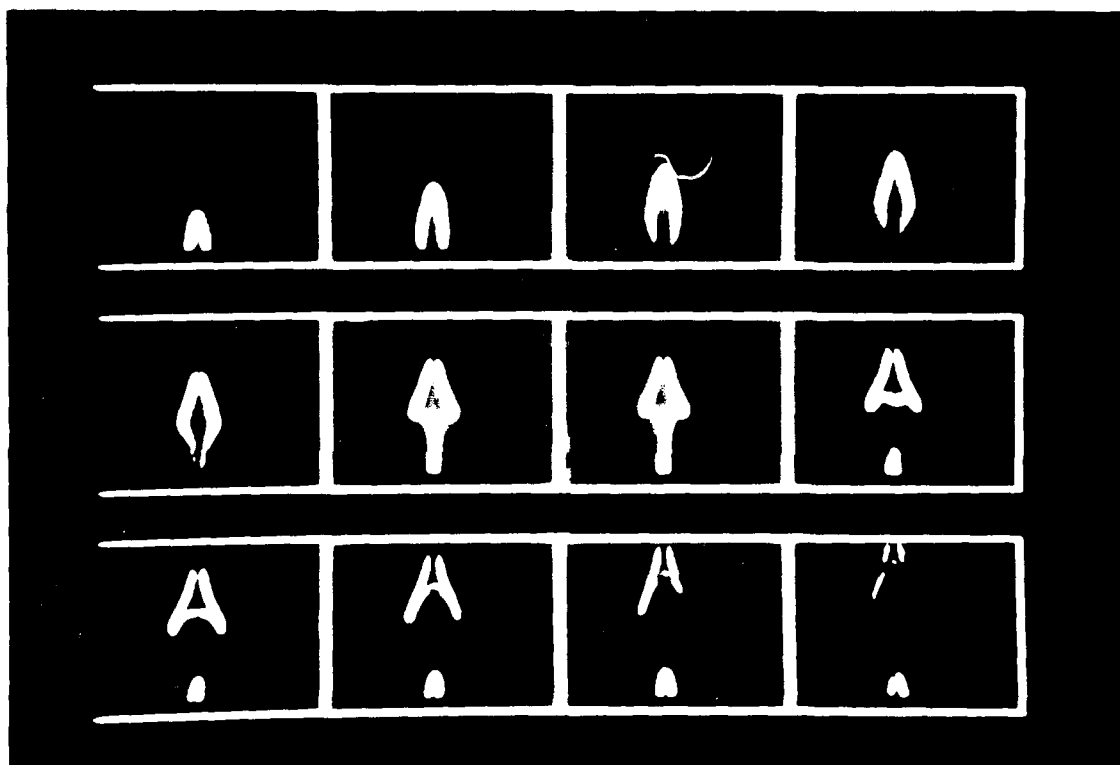
Figure 14. Two-dimensional imaging results from
soot particles formed in a methane/air
diffusion flame at 2 atmospheres pressure.
The vertical field of view is approximately
two inches for each frame shown.

This flame system also has the potential to provide a well controlled unsteady flame environment from which to extend the present laminar flame studies. In this respect, it provides a natural bridge to more complicated turbulent flames, in terms of understanding the evolution of soot particles in these more mixing dominated combustion environments. Additionally, the strong coupling of these experiments with appropriate model development offers some unique possibilities for future work.

4.2.3 Flame Modeling

One of the objectives of the present studies is to develop a model appropriate to describe soot formation in diffusion flames. The approach for this work is to extend current models to the present diffusion flame studies. Emphasis in augmenting such models would be the addition of soot particle transport and possibly radiative effects. During the last year, some effort has been directed towards achieving this objective. Specifically, work has proceeded on using the model developed by Mitchell [7] for similar laminar diffusion flames. However, to date, we have been unsuccessful in applying this model to the present flame studies. The problem appears to be in the limited Reynolds number range over which the Mitchell model is applicable. The larger burner diameter and higher flow rates characterizing the flames presently under study exceed the conditions appropriate for this model.

As an alternative, a diffusion flame model developed by Prof. Merkle at Penn State is being considered. This model has recently been validated using velocity and temperature measurements obtained as part of the present research program. The extensive nature of the data base available from these studies has been quite helpful in Prof. Merkle's model validation. We are presently reviewing with Prof. Merkle the possibility of incorporating particle transport and radiation transfer into this model.

Similar potential exists for collaborative efforts with workers at NIST for both the steady and unsteady flame studies. This approach of incorporating the results of the present studies with the efforts of an on-going modeling effort seems most appropriate for the present studies.

4.3. Conclusions and Future Work

The efforts over the past year have focused on fuel structure effects on soot particle inception and surface growth. In particular, studies of the early particle inception process have shown a strong correlation between large hydrocarbon species observed using laser fluorescence techniques and the amount of soot formed in the flame. These results can potentially be utilized for qualitative comparison with chemical kinetic models capable of predicting hydrocarbon concentrations under fuel rich combustion conditions. However, the present results do not provide quantitative information on the key precursor species nor species specific identification. This must continue to be a major objective for studies of soot formation, since an increasing body of information points to particle inception as the key step in determining the ultimate soot concentration achieved in the flame.

In the present studies, two approaches are under development to address this task. One involves the use of spectral absorption measurements to further quantify the gas phase species present in the preparticle zone. This technique relies on the general correlation that hydrocarbons shift their primary absorption wavelength to longer wavelengths as their mass increases. This procedure is likely to add information to our understanding of the general distribution of mass in the precursor zone, but may not provide further species specific information.

A second approach, which holds strong potential for obtaining more specific quantitative data, involves the use of mass spectrometric sampling from the flame. Under support from the Defense-University Research Instrumentation Program, a mass spectrometer is being acquired for these studies. This instrumentation will be used to study specifically changes introduced by fuel molecular structure variations in the preparticle region of these well characterized diffusion flames. These studies are aimed at providing a more detailed data base relating to the concentration of key soot precursor species in these flames.

Experiments conducted on a series of C_4 fuel species have further established that the surface growth process is largely independent of fuel molecular structure. These studies carried out in a methane baseline flame confirm similar studies previously conducted for ethene baseline flames. These studies quantitatively establish that once available surface area is taken into account, that surface growth rates are substantially independent of the fuel structure or the baseline flame system. These results highlight the importance of understanding the particle inception process which controls the initial available surface area.

Future work needs to focus on two specific questions. The first involves a determination of which species are participating in the surface growth process in diffusion flames. The second concentrates on identifying the process which terminates surface growth. Both decreased surface reactivity with particle aging and oxidative competition represent viable alternatives. Potential approaches to these problems involve in-flame intrusive sampling for major species measurements or laser induced fluorescence measurements of oxidizing species such as OH. Both of these approaches have serious practical problems related to sampling and measurement in particle laden flows. Both remain of interest for future work in this laboratory. In particular, the extension of the mass spectrometric sampling technique discussed above, represents an approach of direct interest, if a suitable probe sampling approach can be developed. Presently, efforts at developing electrically charged probes for soot particle repulsion have shown some promise in studies conducted in the region above the flame itself.

In addition to the above studies conducted in atmospheric flames, high pressure flame studies have also been initiated during the past year. Initial studies using an ethene/air flame system have provided independent verification of previous high pressure diffusion flame studies of soot formation. These studies are presently being extended to a wider range of fuels in order to examine the effects of molecular structure on the observed pressure dependence. Studies of fuel structure effects at elevated pressure will be a major emphasis of the program over the next year.

In the process of these high pressure flame studies, an interesting flame instability phenomena has been observed and studied. Combined experimental and theoretical approaches have been developed in conjunction with workers at NIST to examine the mechanism of flame instability generation. The present experimental facility offers some unique capabilities in terms of isolating buoyancy effects in jet flames. This area is presently being assessed for future work in terms of flame instabilities as well as for studying soot formation under unsteady conditions.

The above results reflect the present state of progress in our understanding of soot formation. The detailed information forthcoming from these and other studies, is providing a framework from which to address specific mechanistic questions. Challenges to further understanding of the soot formation process are limited by our present diagnostic capabilities and future progress will hinge on careful development of measurement approaches. Additionally, significant progress may be forthcoming in areas in which little study has been directed. These include the area of high pressure flames where many questions remain.

5. REFERENCES

1. Jackson, T. A., J. Energy, 6, p. 376 (1982).

2. Blazowski, W. S., Sarofim, A. F. and Keck, J. C., J. of Eng. Power, 103, p. 42 (1981).

3. Santoro, R. J., Semerjian, H. G. and Dobbins, R. A., Combustion and Flame, 51, p. 208 (1983).

4. Santoro, R. J., Semerjian, H. G., Twentieth Symposium (International) on Combustion, The Combustion Institute, Pittsburgh, PA, pp. 997-1006 (1984).

5. Santoro, R. J., Yeh, T. T. and Semerjian, H. G., in Heat Transfer in Fire and Combustion Systems, edited by C. K. Law, Y. Jaluria, W. W. Yuen, K. Miyasaka, pp. 57-69, The American Society of Mechanical Engineers, New York (1985).

6. Glassman, I and Yaccarino, P., Eighteenth Symposium (International) on Combustion, The Combustion Institute, Pittsburgh, p. 1175 (1981).

7. Mitchell, R. E., Sarofim, A. F. and Clomburg, L. A., Combustion and Flame, 37, p. 227 (1980).

8. Dobbins, R. A. and Mulholland, G. W., Combust. Sci. and Tech., 40, p. 175 (1984).

9. Davis, R. and Baum, H., Center for Chemical Engineering, National Bureau of Standards (private communication).

10. Santoro, R. J., Semerjian, H. G., Emmerman, P. J., Goulard, R., Int. J. Heat Mass Transfer, 24, pp. 1139 (1981).

11. D'Alessio, A., DiLorenzo, A., Sarofim, A. F., Beretta, A., Masi, S., And Venitozzi, C., Fifteenth Symposium (International) on Combustion, The Combustion Institute, Pittsburgh, PA, p. 1427 (1975).

12. Dobbins, R. A., Santoro, R. J. and Semerjian, H. G., Ed. T. D. McCay and J. A. Roux, Progress in Astronautics and Aeronautics, Vol. 92, p. 208 (1984).

13. Gomez, A., Sidebotham, G. and Glassman, I., Combustion and Flame, 58, 45 (1984).

14. Gordon, S and McBride, B. J., Computer Program for Calculation of Chemical Equilibrium, NASA, 1984.

15. Santoro, R. J., Yeh, T. T., Horvath, J. J. and Semerjian, H. G., Combustion Science and Technology, 53, p. 89 (1987).

16. Santoro, R. J., "Fuel Molecular Structure Effects on Soot Particle Growth in Diffusion Flames," Twentieth Fall Technical Meeting of the Eastern Section of the Combustion Institute, Gaithersburg, MD, Nov. 2-5, 1987.

17. Haynes, B.S., Jander, H. and Wagner, H. Gg., Ber. Bunsenges. Phys. Chem., 84, 585 (1980).

18. Miller, J. H., Mallard, W. G. and Smyth, K. C., Combust. Flame, 47, 205 (1982).

19. Garo, A., Lahaye, J. and Prado, G., Twenty-first Symposium (International) on Combustion, The Combustion Institute, 1986, pp. 1023-1031.

20. Gomez, A., Littman, M. G. and Glassman, I., Combust. and Flame, 70, 225 (1987).

21. Harris, S. J. and Weiner, A. M., _Combustion Science and Technology_, 31, 155 (1983).

22. Harris, S. J. and Weiner, A. M., _Combustion Science and Technology_, 32, 267 (1983).

23. Frenklach, M., Clary, D. W., Gardiner, W. C. and Stein, S. E., _Twentieth Symposium (International) on Combustion_, The Combustion Institute, 1984, pp. 887-901.

24. Sangiovanni, J. J., "Soot Formation Characteristics of Synthetic Liquid Fuels in Spray Flames," United Technology Research Center Report No. R83-956185.

25. Flower, W. L., _Combustion Science and Technology_, 48, 31 (1986).

26. Flower, W. L. and Bowman, C. T., _Combustion Science and Technology_, 53, 217 (1987).

27. Flower, W. L. and Bowman, C. T., _Twenty-First Symposium (International) on Combustion_, The Combustion Institute, 1986, pp. 1115-1124.

28. Toong, T. Y., Salant, R. F., Stopford, J. M. and Anderson, G. Y., _Tenth Symposium (International) on Combustion_, The Combustion Institute, 1965, pp. 1301-1313.

29. Kimura, I., _Tenth Symposium (International) on Combustion_, The Combustion Institute, 1965, pp. 1295-1300.

30. Buckmaster, J. and Peters, N., _Twenty-First Symposium (International) on Combustion_, The Combustion Institute, 1986, pp. 1829-1836.

31. Lewis, G. S., Cantwell, B. J., Vandsburger, V., and Bowman, C. T., _The Twenty-Second (International) Symposium on Combustion_, The Combustion Institute (in press).

6. PUBLICATIONS

1. Santoro, R. J., Yeh, T. T., Horvath, J. J. and Semerjian, H. G., "The Transport and Growth of Soot Particles in Laminar Diffusion Flames", Combustion Science and Technology, 53, 89 (1987).

2. Solomon, P. R., Best, P.E., Carangelo, R. M., Markham, J. R., Chien, P., Santoro, R. J. and Semerjian, H. G., "FT-IR Emission/Transmission Spectroscopy for In-Situ Combustion Diagnostics", Twenty-first Symposium (International) on Combustion, The Combustion Institute, 1986, pp. 1763-1771.

3. Santoro, R. J. and Miller, J. H., "Soot Particle Formation in Laminar Diffusion Flames", Langmuir, 3, p. 244-254 (1987).

4. Santoro, R. J., "Optical Measurements of Soot Particles in Flames," Mat. Res. Soc. Symp. Proc., Vol. 117, p. 157 (1988).

5. Santoro, R. J., Horvath, J. J. and Semerjian, H. G., "Surface Growth Processes for Soot Particles in Diffusion Flames: Fuel Effects", to be submitted to Combustion and Flame.

7. MEETINGS AND PRESENTATIONS

1. "The Effect of Fuel Structure on the Formation and Growth of Soot Particles in Diffusion Flames", The Twenty-third Biennial Conference on Carbon, Worcester Polytechnic Institute, July 19-24, 1987.

2. "Soot Particle Formation in Diffusion Flames", American Chemical Society Symposium on Advances in Soot Chemistry, ASC Symposium, New Orleans, LA, August 30-September 4, 1987.

3. "Fuel Molecular Structure Effects on Soot Particle Growth in Diffusion Flames", Twentieth Fall Technical Meeting of the Eastern Section of the Combustion Institute, Gaithersburg, MD, November 2-5, 1987.

4. "Optical Measurements of Soot Particles in Flames", Materials Research Society Symposia, Reno, Nevada, April 5-8, 1988.

5. "Soot Growth in Diffusion Flames Burning Fuel Mixtures", 1988 Fall Technical Meeting of the Eastern Section of the Combustion Institute, Clearwater Beach, FL, December 5-7, 1988.

6. "Optical Measurements of Soot Particles in Flames," Wright Patterson Air Force Base, Dayton, Ohio, March 6, 1989.

7. Invited Attendee for the Round Table Discussion on "Current Problems in Soot Formation During Combustion," The Commission on Condensation Phenomena of the Academy Science, Gottingen, Germany, March 29 and 30,1989.

8. PARTICIPATING PROFESSIONALS

Dr. Robert J. Santoro, Associate Professor of Mechanical Engineering
Mr. Rahul Puri, Graduate Student, Department of Mechanical Engineering
Mr. Jeff Leet, Graduate Student, Department of Mechanical Engineering
Mr. Thomas Richardson, Graduate Student, Department of Mechanical Engineering
Mr. John Ness, Graduate Student (AFRAPT), Department of Mechanical Engineering

9. INTERACTIONS

A number of researchers have directly used the extensive data set developed as part of this work to compare with or extend their own research. Some of those who have been directly provided data include:

Professor R. A. Dobbins, Brown University, Providence, RI
Dr. R. Hall, United Technologies Research Center, East Hartford, CT
Dr. R. Davis, The National Bureau of Standards, Gaithersburg, MD
Dr. P. Solomon, Advanced Fuel Research, Inc., East Hartford, CT
Dr. I. Kennedy, University of California, Davis, CA
Drs. C. Merkle and S. Turns, The Pennsylvania State University, University Park, PA

In addition to the interactions resulting from interest in the soot particle data, there have been interactions with researchers on particle diagnostic problems. In some cases this has resulted in direct visits to particular laboratories to assist in solving these problems. These interactions include:

Dr. M. Zachariah, The National Bureau of Standards, Gaithersburg, MD
Ms. Valerie Lyons, NASA Lewis Research Center, Cleveland, OH

Several other interactions have also occurred through a general interest in the work supported by AFOSR with:

Columbian Chemical Company, Monroe, LA
Cummins Engine Company, Columbus, IN
DuPont